# OPTIMAL DISPATCH OF MOBILE STORAGE UNIT TO SUPPORT EV CHARGING STATIONS

by

Mohamed Mostafa Abdelazim Elmeligy

A Thesis presented to the Faculty of the
American University of Sharjah
College of Engineering
In Partial Fulfillment
of the Requirements
for the Degree of

Master of Science in
Electrical Engineering

Sharjah, United Arab Emirates

April 2021

**Declaration of Authorship**

I declare that this thesis is my own work and, to the best of my knowledge and belief, it does not contain material published or written by a third party, except where permission has been obtained and/or appropriately cited through full and accurate referencing.

Signed: **Mohamed Mostafa Elmeligy.**

Date: **26/04/2021.**

The Author controls the copyright for this report.

Material should not be reused without the consent of the author. Due acknowledgement should be made where appropriate.

© Year 2021

Mohamed Mostafa Abdelazim Elmeligy

ALL RIGHTS RESERVE

## Approval Signatures

We, the undersigned, approve the Master's Thesis of Mohamed Mostafa Elmeligy

Thesis Title: Optimal Dispatch of Mobile Energy Storage Unit to Support EV Charging Stations.

Date of Defense: 20/04/2021

| **Name, Title, and Affiliation** | **Signature** |
|---|---|
| Dr. Mostafa Shaaban<br>Associate Professor, Department of Electrical Engineering<br>Thesis Advisor | |
| Dr. Mohamed Hassan<br>Professor, Department of Electrical Engineering<br>Thesis Committee Member | |
| Dr. Maher Azzouz<br>Assistant Professor, Department of Electrical and<br>Computer Engineering<br>University of Windsor<br>Thesis Committee Member | |
| Dr. Nasser Qaddoumi<br>Head or Program Coordinator<br>Department of Electrical Engineering | |
| Dr. Lotfi Romdhane<br>Associate Dean for Graduate Affairs and Research<br>College of Engineering | |
| Dr. Sameer Al-Asheh<br>Interim Dean<br>College of Engineering | |
| Dr. Mohamed El-Tarhuni<br>Vice Provost for Graduate Studies<br>Office of Graduate Studies | |

**Acknowledgement**

I would like to thank my advisor Dr. Mostafa Shaaban for his continuous support, teachings, guidance, patience, and motivation throughout the different stages of this research. I'm deeply beholden for his great assistance, worthy discussion and suggestions.

I want to express my gratefulness to Dr. Mohamed Mokhtar from Ain Shams University, Dr. Maher Azzouz, and Dr. Ahmed Azab from University of Windsor for their great assistance and undeniable support throughout this research.

I would like to thank the professors of the Electrical Engineering department who taught me the master level courses with mighty teaching methods and skills. I am appreciating their dignified pieces of advice and motivation. I'm thankful for all I learned from all of you. I would like to acknowledge the graduate assistantship provided by American University of Sharjah that made me able to complete this thesis.

## Dedication

To my family, thank you for all the support you have shown me through this journey. Special thanks to my loving parents, Mostafa and Ebtisam, for their wise counsel and sympathetic ear, you were always there for me. Finally, I could not have completed this thesis without the support of my brothers, Ahmed and Abdulrahman, who provided words of encouragement as well as happy distractions to rest my mind outside of this work.

## Abstract

As transportation electrification increases globally, new technologies emerged in the past few years to meet the growth of the electricity demand. A mobile energy storage system (MESS) could provide several services to the distribution systems such as reactive power support, renewable energy integration, peak shaving, and load leveling. In addition, an MESS can be utilized to support electric vehicles (EVs) charging in different parking lots (PLs), which is the main focus of this thesis. The task of multiple stationary storage units can be achieved using a single MESS with a relatively lower cost. In this thesis, a new dynamic optimal dispatch strategy for MESS is proposed to support several charging stations sharing the same geographical area. The objective of the proposed approach is to optimally dispatch the MESS in conjunction with optimal EVs charging to minimize the total operation cost and address the extra demand of PLs. Different case studies are provided on the IEEE 38-bus system and a real radial feeder in Ontario, Canada to test the proposed approach. In the second phase of this research, a new approach is proposed for the optimal resource allocation for an MESS fleet owned by multiple PLs sharing the same geographical area and sharing its capital and operational cost. The aim is to optimally decide on the number of MESSs and their battery bank capacities that should be used in order to serve charging stations participated in the project. The optimization includes practical constraints for battery dynamics. Comparative case studies showed the effectiveness of the proposed algorithms.



**Keywords: Mobile Storage Unit; Battery-based energy storage system; Electric Vehicles; Charging stations; Mathematical Modeling and Programming.**

## Table of Contents

## List of Figures

## List of Tables

## List of Abbreviations

| | |
|---|---|
| CDF | Cumulative Density Function |
| CS | Charging Station |
| DG | Distributed Generation |
| DSM | Demand Side Management |
| DTSP | Dynamic Travel Salesman Problem |
| EMS | Energy Management System |
| ESS | Energy Storage System |
| EV | Electric Vehicle |
| FCFS | First-Come-First-Served |
| G2V | Grid-to-Vehicle |
| MESS | Mobile Energy Storage System |
| MINLP | Mixed-Integer Non-Linear Programming |
| PDF | Probability Density Function |
| PF | Power Flow |
| PV | Photo-Voltaic |
| PL | Parking Lot |
| RES | Renewable Energy Resources |
| TSP | Travel Salesman Problem |
| V2G | Vehicle-to-Grid |

# Chapter 1. Introduction

## 1.1. Overview

Due to the exponential increase in transportation electrification and the trend of going green, the electricity demand is rapidly increasing. Distribution systems are witnessing high demand that might not be able to accommodate, especially in the urban areas that require a relatively high cost to upgrade the grid infrastructure. The exponential market growth of electric vehicles (EVs) reflects a high demand, which is projected to reach up 27 million units in 2030 compared to 3.5 million in 2020 [1], this is due to many reasons such as the reduction in CO2 emissions, the possibility of using the batteries as storage elements, and the significant reduction of batteries prices [1-2]. This dramatic increase in EVs will result in huge challenges to the reliability of power systems to address this demand since EVs will represent large loads and could further result in significant stress on the distribution systems [2]. As a result, the EVs' charging behavior control is a must. On the other hand, higher penetrations will cause a voltage rise during low demand hours [3] and EV charging coordination may be the solution to decrease the voltage fluctuation. Electric utilities must conduct proper management for EVs by applying Demand Side Management (DSM) programs which proved their effectiveness in load shifting to off-peak times and peak shaving, EVs might be a burden or a plus depending on the charging behavior.

## 1.2. Thesis Motivation

Future power grids will witness a shift in focus to install Energy Storage Systems (ESS) since it can introduce flexibility to the system. ESS could be used efficiently to increase the proper use of modern energy resources including Renewable Energy Resources (RES) by contributing to almost stable power output and storing extra unused power to avoid curtailment, which can accommodate the increasing demand of power without compromising on the minimization of CO2 emissions. The installation of ESS can also provide voltage support through VAR compensation [4]. We are at the very primitive stages of using ESS and maximizing its benefits. It was the norm in all previous studies to provide a stationary solution either by coordinate the EV charging or using stationary suppliers like Distributed Generation (DG) units and batteries. However, using a Mobile Energy Storage System (MESS) will lead to a

significant reduction in the implementation cost. Especially if multiple parking lots are sharing the same geographical area.

## 1.3. Research Contribution

The listed points summarize the thesis contribution as follows:

- Proposing a new approach to optimally dispatch an MESS in conjunction with optimal EV charging to address the extra demand of distributed EV charging stations,
- Developing a new integrated scheduling and sequencing approach to decide on the optimal order and the period spent at each PL,
- Constructing a detailed simulation of a typical distribution system to show the effectiveness of the proposed approach,
- Proposing a planning algorithm for several MESSs to serve multiple EVs charging stations while accounting for the uncertainties, and
- Applying a probabilistic model to generate various virtual scenarios of PV output power using limited historical data.

## 1.4. Thesis Organization

The chapters of this thesis are organized as follows:

- **Chapter 2** discusses the background and literature related to the EVs demand solutions, MESS previous work, and implementation of different DTSP models.
- **Chapter 3** presents the integration of an MESS to support and serve multiple EVs charging stations.
- **Chapter 4** discusses the optimal dispatch of a mobile storage unit to support EV charging stations.
- **Chapter 5** proposes optimal planning of several MESSs to serve multiple EVs charging stations.
- **Chapter 6** concludes these presented algorithms along with ideas for future work.

# Chapter 2. Background and Literature Review

To fully understand the motivation, objectives, and the purpose of the work done in this research, we must have a clear vision of the components and the technologies that have emerged recently which made the designing and modeling of MESS is necessary. In this chapter, an overview of EVs' demand accommodation will be summarized in order to give the reader a better understanding of the full system. The light must be shed on ESS technology and its benefits, especially MESS which is the main focus of this thesis. The definition, types, and variants of DTSP are discussed as well.

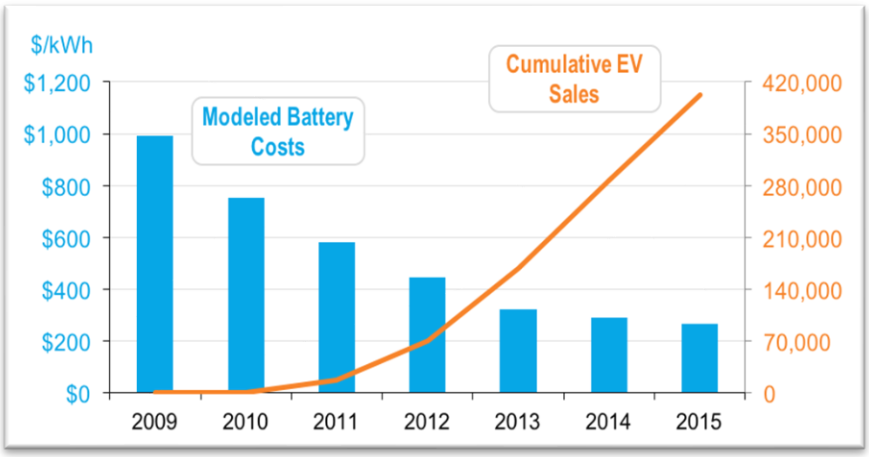


Figure 2.1 Modeled battery costs related to increasing EV sales [5].

## 2.1. Electric Vehicles (EVs)

The new evolving technologies of smart grids across the world will enhance the utilization of electric vehicles as part of the grid. EVs can be a burden or a plus depending on the charging behavior. One of the most important aspects of EVs evolving is the possibility of using its batteries as storage elements. Through the concept of vehicle-to-grid (V2G), EVs will act as a part of the storage system connected to the network and providing power where the vehicle is located. The V2G concept will allow the EVs to trade power with the grid during on-peak and off-peak hours. For instance, a vehicle can charge during off-peak hours and discharge its power during the on-peak time of the day. This will result in a benefit for the EV owner since he might get some profit, in addition to helping the grid to supply the power in peak hours. This idea will be a great addition to the power systems due to the rapid increase in EVs sales in the last 10 years. This increases due to many reasons, for example, the trend of going green,

minimizing CO2 emissions, and the batteries dropping prices. Figure 2.1 shows a comparison of the number of EVs compared to the price of batteries. It is extremely important to mention that this cycle depends mainly on the driving profile of the owner which is might not suitable for everyone.

Like MESS, EVs can be used in order to participate in grid activities and supply power in on-peak demand and selling prices time; however, using EVs will not be reasonable due to uncontrollable availability time [6]. Also, the unwillingness of all the EVs owners to participate in the grid [7]. Moreover, a high number of EVs is required to replace only one MESS truck. EVs can be categorized into three groups: Battery Electric Vehicle (BEV), Hybrid Electric Vehicle (HEV), and Fuel Cell Electric Vehicle (FCEV). The characteristics and differences of each type are as follows:

- *Battery Electric Vehicle (BEV)*: All the power demanded functions of the vehicle are supplied through a full electrical propelling system, unlike the other types mentioned below. The battery capacity of this type of vehicle determines the mile range which should be increased in order to meet all demands. A properly designed charging station is used in order to fully charge this battery type. The most popular example developed by Tesla Motors, which provides a driving range of 300 mi per charge and consists of a Li-ion battery pack [8].

- *Hybrid Electric Vehicles (HEV)*: This type of vehicle act like an electrical machine, it has a battery to store energy and an internal combustion engine that produces the main source of power [9]. There are different levels of HEVs like Micro HEV which has a limited power electric machine used as a starter only. It increased the fuel economy from 2% to 10% using this technique. The Mild HEV adds up another level to the previous one which a boost function to the vehicle, resulting in a supplementary torque during the breaking or acceleration process. Fuel economy has shown a 10% to 20% improvement. The fully hybrid vehicle implements a full electric traction system inside the vehicle resulting in a zero-emission automobile. The fuel economy at this level reached up to 50%. Finally, the Plug-in HEV uses an external charging station to fully charge the battery. The internal combustion engine can be used to charge the battery as well, but if ICE is not charging the battery, the fuel economy can record 100%

improve which makes this level of HEV a very important topic to focus on in the market.

- *Fuel Cell Electric Vehicle (FCEV)*: This type can be considered as a variation of BEV since the fuel cell can work as a generator using hydrogen as fuel and oxygen as oxidant while storing the energy in the battery. Many fuel sources can be used, for example, alcohols and hydrocarbons. But hydrogen is preferred due to that its byproduct is just water plus it has a high energy density [8].

A summary of the different types of EVs is presented in Table 2.1.

Table 2.1 Summary of EV specifications [9].

| | **Energy Source** | **ESS** | **Characteristics** |
|---|---|---|---|
| **HEV** | Gas stations<br>electric grid charging stations | Fuel tank<br>battery | Low emissions<br>High fuel economy |
| **BEV** | electric grid charging stations | Battery | Zero emissions<br>Independent of fossil fuels |
| **FCEV** | Hydrogen<br>other possible fuels | Hydrogen tank<br>battery | Zero emissions<br>Independent of fossil fuels (if not using gasoline to produce H2) |

## 2.2. Energy Storage Systems (ESS)

ESS plays a vital role in the electric network, especially in the case of smart grid technologies implementation. As seen in Figure 2.2, the cost associated with different battery types has dropped through the past few years and it is expected to decrease more and more during the next few years. ESS can be categorized based on different criteria. It can be subcategorized based on the form of stored energy; i.e., mechanical, chemical, or electrical. While electrical storage can be subdivided into magnetic energy storage and electrostatic storage, mechanical storage also can be divided into potential energy storage and kinetic energy storage [10]. Another criterion is the charging/discharging time. The centralized bulk units can store a high amount of energy reaching up to hundreds of megawatts for more than 8 hours, known as long-term ESS. On the other

hand, the short-term ESS is used for a shorter time with a relatively smaller energy amount [10].

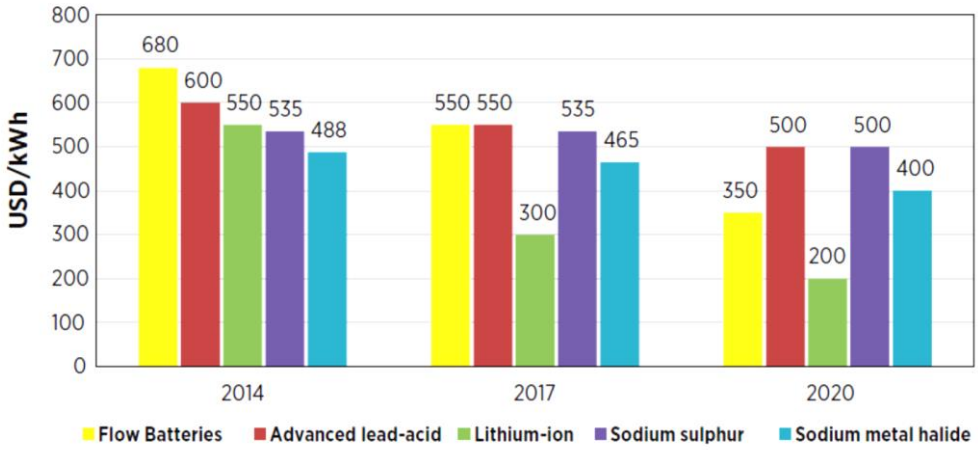


Figure 2.2 Price drop for different types of batteries [11].

Some types of ESS are briefly discussed below:

- *Battery Energy Storage System (BESS)*: This is the most common form of ESS, batteries can vary in their storage capacities taking into consideration other factors based on different applications. Lead Acid batteries, Lithium-Ion batteries, and Oxy-Hydroxide batteries are examples of BESS.
- *Compressed Air Energy Storage (CAES)*: Energy is stored in form of air during off-peak hours. When demand is high, compressed air is heated to move a turbine shaft and generate the required power at that time.
- *Flywheel Energy Storage System (FESS)*: In this type, energy is stored in form of kinetic (mechanical) energy. A large rotating wheel forms the flywheel and the amount of energy stored changes linearly with the rotational speed and with the inertia of the flywheel.

The ESS units are widely used due to several benefits, they can reduce the dependency on fossil fuels, providing the required power without compromising on minimizing the CO2 emission, participating in cost reduction by supplying power in on-peak demand, and resulting in avoiding the extra generators at this time, helping distribution and transmission networks to be more stable, and maximizing the usage of the existing generating units and RES units in particular [12]. A summary of important characteristics of different types of ESSs are summarized in Table 2.2.

Table 2.2 Characteristics of different ESS types [13].

| Type | Energy Efficiency (%) | Energy Density (Wh/kg) | Power Density (W/kg) | Cycle life (cycles) | Self-Discharge |
|---|---|---|---|---|---|
| **Pb-Acid** | 70-80 | 20-35 | 25 | 200-2,000 | Low |
| **Ni-Cd** | 60-90 | 40-60 | 140-180 | 500-2,000 | Low |
| **Ni-MH** | 50-80 | 60-80 | 220 | <3,000 | High |
| **Li-ion** | 70-85 | 100-200 | 360 | 500-3,000 | Med |
| **Li-polymer** | 70 | 200 | 250-1,000 | >1,200 | Med |
| **NaS** | 70 | 120 | 120 | 2,000 | - |
| **VRB** | 80 | 25 | 80-150 | >16,000 | Negligible |
| **EDLC** | 95 | <50 | 4,000 | >50,000 | Very high |
| **Pumped hydro** | 65-80 | 0.3 | - | >20 years | Negligible |
| **CAES** | 40-50 | 10-30 | - | >20 years | - |
| **Flywheel (steel)** | 95 | 5-30 | 1,000 | >20,000 | Very high |
| **Flywheel (composite)** | 95 | >50 | 5,000 | >20,000 | Very high |

## 2.3. Mobile Energy Storage Systems (MESS)

The ESS can be mobilized in order to serve different locations at different times, in that can it called MESS. It is a transportable energy system that provides several benefits to the grid. The most common type of batteries used for MESS is Lithium-ion to store and carry power along with other different components which could include the following:

- Other Generation Sources: Like Diesel Generators, Fuel cells, or PV panels.
- Power Electronic Circuits: Converters and inverters are needed in the conversion process from DC (RES outputs) to AC currents to serve the required loads.
- Energy Management Systems (EMS): In the case of multiple storage elements, an EMS would be useful to control the power flow and maximizing power usage.
- Mobility: Different kinds of mobility could be used; however, it could be a normal ESS fixed on a truck or on a shipping container to achieve mobility.

Different companies are providing commercial mobile energy storage units with an output power of different ratings like 100, 1000, and 5000 kW. Various projects around the world have used MESS. Toshiba and the Spanish Company Gas Natural Fenosa have tested Toshiba's BESS which consists of lithium-ion battery packs providing 500 kW of power. They studied the effect of the system on voltage and frequency stability of the grid at different sites as well as peak shaving capability [14].

**2.3.1 Benefits of MESS.** Being able to travel and connect to the grid at different times and locations is a great advantage that provides various services to the grid. Besides the relatively lower cost of MESS that can replace multiple stationary ESS, a few benefits are listed below.

***2.3.1.1 Voltage support***. Maintaining a stable voltage level within the system's limits is a crucial aspect of a stable power system. The centralized generation sources can supply the compensation of the extra reactive power required by inductive or capacitive loads. The most common power factor correction method is using capacitor banks, but the problem can be seen in the power loss since capacitor banks withdraw a huge amount of current while operating. The installation of ESS can be used in this manner but it is really expensive to install many ESSs; however, MESS can do the job of multiple stationary ESS since it can change location easily and serve as needed.

***2.3.1.2 RES balancing.*** It is well known that RES units can provide a clean source of energy, but it faces some problems when being part of the system. The control process of the output is really difficult [15]. PV output could vary a lot due to the effect of shading, and strong winds can affect the output of a wind generator. This problem results in unstable output power from these units. As a solution, RES units often come with ESS installed in order to store the unused generated power. This combination can guarantee an almost constant output power. However, providing a suitable ESS can add to the costs of the systems especially with the increased penetration of RES generators. The increased demand for MESS and PEV will reflect a reduction in the price of these units and making them more economically attractive than the normal stationary ESS. MESS can be located on the buses that have RES generators to offset their production.

**2.3.2 Applications of MESS.** MESSs are used in many applications, a brief of each application is summarized as follows:

***2.3.2.1 Peak shaving.*** Peak shaving refers to any method used to reduce the power consumption during the peak hour in order to maintain a better peak-to-average ratio. Prior to the DG units, utilities would build a new power plant in order to serve during this short-time demand. Instead, utilities might force customers to cut down their loads in these peak hours or charge a higher cost for example. However, this is a huge problem for customers, especially in industrial areas. A mobile DG unit might be the perfect solution in this case since it can travel to serve during these on-peak hours**.**

***2.3.2.2 Short-term events.*** Many events are placed in order to take place once a year or festivals that expect many visitors during a short period. Those events last for few hours and required a huge amount of power to supply the needed demand. An MESS can take place in order to provide the necessary power to hold these events without stressing the grid.

***2.3.2.3 Remote areas or refugee camps.*** Due to wars, more and more people are seeking refuge in United Nations camps. Since these camps usually built-in areas away from transmission lines and distribution networks, a standalone MESS is an excellent solution to provide such areas with the required power for a limited period of construction or power outage. It might be a great solution for construction sites that requires a lot of energy 24 hours a day while building a new city for example away from distribution lines**.**

***2.3.2.4 Natural disaster crisis.*** The number of natural disasters is increasing over time; floods, earthquakes, wildfires, cyclones, hurricanes. The occurrence of those events can cause severe damage to the urban area's generation units and infrastructure which might directly affect the recurring process and leave millions of people in a complete blackout. MESS in this case can help supply specific areas until the main grid is back in action. The mobility aspect is beneficial in this case since multiple areas can be served accordingly upon need.

## 2.4. Demand Side Management (DSM)

Demand Side Management is usually used to refer to a group of actions specifically designed to control and manage a utility's energy consumption and power demand in order to get a more reliable demand curve that increases the reliability and stability of generation and distribution systems. The aim is to modify the demand profile concerning the overall consumption curve. To engage a DSM program, a detailed analysis should take place first to highlight the areas of improvement possibilities. In case a not feasible supply or not sufficient reduction cost achieved, the on-site installation of the following can take place:

- Batteries (BESS)
- Mobile Energy Storage System (MESS)
- RES units (photovoltaic, wind)
- Cogeneration systems.

DSM can be used in order to accomplish different load shaping objectives, such as peak clipping or shifting. Another objective is to get a flexible load shape or applying strategic conservation or load grwth as seen in Figure 2.3.

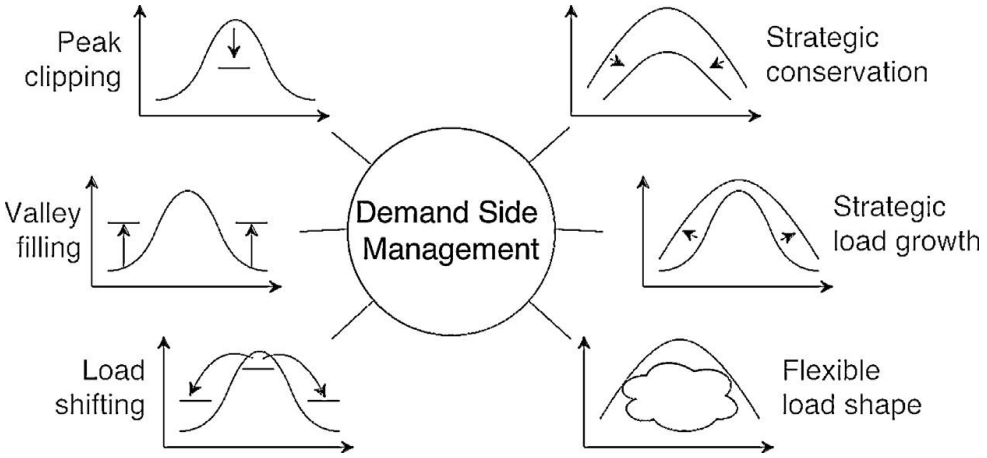


Figure 2.2 Basic load shaping techniques [16].

## 2.5. Literature Review

To understand the work being done in this field until now, a search was conducted to further enrich our thought in applying our methodology in the three different fields involved in this research. First, we will explore some EVs demand solutions to accommodate this increasing power demand. Followed by a related work

of MESS and application. Finally, different variants and definitions of DTSP will take place.

**2.5.1 EVs demand accommodation.** As EVs are increasing dramatically in the market, it requires a lot of power in order to charge these EVs which puts stress on the distribution network. Recently, several researchers have studied multiple solutions to reduce the peak hour demand and improve power quality (e.g., line flow constraint, transformer capacity constraint, etc). To minimize EVs charging effect on customer preferences, a demand response strategy is proposed in [17]. In [18], EVs are used to reduce the demand at peak hours as a bidirectional power source. However, this strategy raised a concern about the battery wear and the effect of using EVs for providing base-load power which is discussed in [19]. Vehicle-to-grid (V2G) strategy proposed in [20] is a solution that is not considered in this paper. In [21], an adaptive EV charging scheduling framework is proposed while satisfying network constraints. A management scheme for effective installation and utilization of photovoltaic (PV) is discussed in [22].

In [23], a single house case study is presented to implement DSM using EV batteries as storage elements. In [24], a multi-objective optimization problem is formulated based on a heavy communication between the hub and the distribution utility to optimally coordinate EVs charging. The impact of demand response strategies on smart households' load took place in [25] applying the optimal appliance scheduling considering electricity price variations. A decentralized fuzzy-based controller is introduced in [26] in order to coordinate the charging of EVs that meet the constraints. In [27], a hierarchical distributed energy management for EV charging stations is proposed aimed to maximize the charging power. Two different energy management schemes are proposed in [28] and [29] aiming to reduce the load demand and load fluctuations on the system by optimizing EVs charging power. An algorithm aiming to reduce the operational cost while maximizing customer satisfaction by scheduling the charging and discharging operations is proposed in [30]. It is an optimization and control algorithm for charging stations equipped with PV generation and fixed energy storage that tries to balance the supply and demand by scheduling the charging and discharging operations. In [31], a stochastic dynamic energy management and pricing scheme for EV charging stations deals with uncertainties-charging demand is

presented. Considering energy storage systems and renewable energy integration, the provided deals with uncertainties-charging demand and electricity price fluctuation. Authors of [32] proposing an energy storage management scheme using a hybrid optimization algorithm that depends on varying electricity prices. A charging station utilized with PV panels, energy storage systems (ESS), and fuel cell systems is presented in [33] with an algorithm for economic dispatch.

**2.5.2 MESS related work.** Like MESS, EVs can be used in order to participate in grid activities and supply power in on-peak demand and selling prices time; however, using EVs will not be reasonable due to uncontrollable availability time [34]. Also, the unwillingness of all the EVs owners to participate in the grid [35]. Moreover, a high number of EVs is required to replace only one MESS truck. In terms of MESS, several investigations took place by Electric Power Research Institute (EPRI) [36]. An energy management system for MESS is proposed in [14], which controls the dispatching of the MESS and scheduling the truck position. The truck provides several services. For example, load shifting, power balancing, and improving demand management results. An operation strategy of MESS is presented in [37] which uses progressive hedging (PH) algorithm. The battery exchange stations (BESs) could be an alternative solution to accommodate EVs' demand and reduce the operational cost; however, it outperforms the conventional charging station [38] in the absence of the MESS which is not the case in this paper.

**2.5.3 DTSP review.** We are proposing a MESS owned by and serves multiple utilities sharing the same geographical area in order to shave the peak demand and minimize the operational cost. To optimally schedule and dispatch MESS, a Dynamic Travel Salesman Problem (DTSP) should be implemented. The deterministic Travel Salesman Problem (TSP) and its various types have been extensively studied due to its important applications in real-world problems (e.g., telecommunications, neuroscience, and logistics) [39]. However, considering arriving times has been limited in the literature and the definition of dynamicity varies among the researchers. In [40], dynamicity has been defined as introducing traffic jam to the distance matrix, which makes the distance matrix varies for each time segment. In [41], the author defined dynamicity as the ability to add and remove cities (nodes) while solving the DTSP on account of varied conditions. [42] proposes a DTSP with stochastic release dates which

means that goods have been supplied to customers after being arrived at the depot. The uncertainty of the arrival times of the goods is the main factor for an efficient distribution process. Authors of [43-44] studied the stochastic TSP with time window constraints (STSPTW) depending on stochastic generated travel and service times. A DTSP is formulated and well-explained in order to be used in a search-and-rescue application proposed in [45].

## Chapter 3. A Mobile Energy Storage Unit Serving Multiple EVs Charging Stations

The algorithm presented in this chapter aims at integrating a mobile energy storage system shared by multiple EVs charging stations that are located in the same geographical in order to reduce their peak demand level, which represents a huge part of their monthly operational cost. These PLs having different peak times, which justify the application of a portable ESS (i.e., MESS) to defer the network upgrade and meet the PL demand. Having an MESS that able to move between different locations and from one bus to the other, supplying multiple loads at different times will help reduce the power drawn from the grid. Furthermore, it can be used in serving EV charging stations due to the uncontrolled peak demand period. EVs cannot be easily controlled since the customer can require power at a different time with different daily profiles.

Another solution that provides similar grid services like the MESS is aggregated EVs which does not require any initial cost investment; however, the availability time of the aggregated EVs in PLs is uncontrollable [46] which questions the reliability of the model. Moreover, not all EV owners are willing to participate in such a process. Besides, a large number of EVs is required in order to supply the same power as a single MESS. The following assumption are made in this formulation:

- Customers' requirements are received day-ahead.
- Visiting order of the charging station is known based on the forecasted load profile.

### 3.1. Problem Formulation

To model the problem, the time horizon is defined as 24-time slots a day, each slot is one hour span and represented as a set $t = \{1,2, 3...,24\}$. Transportation time between PLs includes moving between one PL and another, traffic, connecting, and disconnecting times.

The objective function is defined in (3.1), which aims at minimizing the total drained power by the PLs to charge the arrival EVs, as follows:

$$\min \sum_{i} \left( \sum_{t} \left( C_t^{grid} \times P_{i,t}^{EV-Total} \right) \right) \tag{3.1}$$

where $C_t^{grid}$ is the grid cost that varies at each time interval and the total power

consumed by EVs at each bus and each time interval is represented by $P_{i,t}^{ev}$. $i$ is the location of the PL.

**3.1.1 Power flow constraints.** The well-known nonlinear power flow equations are presented in (3.2) and (3.3), in which $\boldsymbol{P_{i,t}^{ev}}$ is added as a load the specified buses, as follows:

$$\frac{P_{i,t}^{G} - P_{i,t}^{L}}{V_{i,t}} = \sum_{j} V_{j,t}\left(G_{i,j}\, cos\, \delta_{i,j} + B_{i,j}\, sin\, \delta_{i}\right) \,, \forall i, t \tag{3.2}$$

$$\frac{Q_{i,t}^{G} - Q_{i,t}^{L}}{V_{i,t}} = \sum_{j} V_{j,t}\left(G_{i,j} \cos \delta_{i,j} + B_{i,j} \sin \delta_{i}\right), \forall i, t \tag{3.3}$$

where $i$ and $j$ denote bus indexes, $P_{i,t}^{L}$ and $Q_{i,t}^{L}$ represent the real and reactive load powers, respectively, $P_{i,t}^{G}$ and $Q_{i,t}^{G}$ are the real and reactive generated power, respectively, $G_{i,j}$ and $B_{i,j}$ represent conductance and susceptance between buses $i$ and $j$, and $V_{i,t}$ and $\delta_i$ represent the voltage and angle level.

The voltage levels have to be maintained within the acceptable limits as expressed in (3.4). Also, the thermal line limits impose an upper limit on the line current magnitude as in (3.5), as follows:

$$V^{min} \leq V_{i,t} \leq V^{max} \qquad \forall\, i, t \tag{3.4}$$

$$I_{i,j,t} \leq I_{i,j}^{max} \tag{3.5}$$

where $V^{min}$ and $V^{max}$ are the minimum and maximum permissible voltage levels in p.u., respectively; $I_{i,j}^{max}$ and $I_{i,j,t}$ is the maximum allowable current and the actual current at time $t$ through the line between buses $i$ and $j$, respectively.

**3.1.2 EV demand constraints.** EVs charging process is presented using (3.6) for each PL. The power delivered to each EV at each time slot depends on the availability of the car in the first place which is indicated by $\boldsymbol{Logic(n,t)}$, i.e., if $\boldsymbol{Logic(n,t) = 1}$, then the car is available in the PL at time $\boldsymbol{t}$ as illustrated in (3.7). Equation (3.8) ensures that every EV is receiving the pre-required demand, while (3.9) computes the total demand of each charging station, as follows:

$$P_{n,t}^{EV} \leq Logic(n,t) \times Ch \,, \forall\, n, t \tag{3.6}$$

$$Logic(n,t) = \begin{cases} 1 \,, Arrival \leq t \leq Departure \\ 0 \,, otherwise. \end{cases} \tag{3.7}$$

$$E_n^{EV-req} = \sum_t P_{n,t}^{EV} \ , \forall\, n \tag{3.8}$$

$$P_{i,t}^{EV-Total} = \sum_n P_{n,t}^{EV} \ , \forall\, i \in \mathbb{I}_{ev}, t \tag{3.9}$$

where $Ch$ is the maximum available charging rate and $n$ is the total number of arrival cars in each PL. $P_{n,t}^{EV}$ is total power delivered to each car $n$ at each time slot $t$. $E_n^{EV-req}$ denotes the demand for each EV. $P_{i,t}^{EV-Total}$ denotes the total consumed power in each PL.

The state of charge (SOC) of each EV is updated with the charging energy as in (3.10) and (3.11):

$$SOC_{n,t} = SOC_{n,t-1} + \Delta SOC_{n,t} \tag{3.10}$$

$$\Delta SOC_{n,t} = \frac{P_{n,t}^{EV} \times \Delta T}{E_n^{BAT}} \tag{3.11}$$

where $SOC_{n,t}$ is the SOC at time $t$ for each EV; $\Delta SOC_{n,t}$ the change in the SOC due to charging; $\Delta T$ is the time segments in hours; $E_n^{BAT}$ represents the battery capacity in kWh.

**3.1.3 Mobile storage modeling.** MESS will supply power only if it is available at the PL; it should visit each location only once. A binary variable is introduced to represent the location of the MESS at each time slot, $\boldsymbol{x_{m,t}}$ as shown in (3.12), where $\boldsymbol{m} = \{\mathbf{1}, \mathbf{2}, \ldots, \boldsymbol{N_m}\}$ and $\boldsymbol{N_m}$ is the total number of charging stations. $\boldsymbol{T_t}$ is another binary variable representing the traveling period. If it is equal to 1, then the MESS is moving from one spot to another, otherwise, it should be zero. The MESS should be available at a PL or traveling between PLs at each time segment.

$$x_{m,t} = \begin{cases} 1 : if\ EV\ is\ availabe\ at\ PL_m\ at\ time\ t \\ 0, otherwise. \end{cases} \tag{3.12}$$

Equation (3.13) ensures that the MESS will be available at one location at a time and (3.14) signifies that the MESS should visit all the PLs during the day.

$$\sum_m x_{m,t} + T_t = 1, \forall\, t \tag{3.13}$$

$$\sum_t x_{m,t} + T_t \geq 1, \forall\, m \tag{3.14}$$

A new binary variable $y_{m,t}$ is introduced in order to capture the change in the state of $x_{m,t}$. As illustrated in (3.15), the variable $y$ computes the change of the present state of variable $x$ from the previous one. By allowing only two changes for each PL as presented in (3.16), we ensure only two state changes to take place and as a result, only one rising edge and one falling edge take place as illustrated in Figure 3.1. Equations (3.15) and (3.16) ensure that variable $x_{m,t}$ have a rectangular pulse; however, the width of the rectangle (time spent at each PL) is to be optimized based on each PL demand.

$$y_{m,t} = (x_{m,t} - x_{m,t-1})^2, \forall\, m, t \tag{3.15}$$

$$\sum_{t} y_{m,t} = 2\ , \forall\, m \tag{3.16}$$

After the departure of the first PL (first falling edge), the MESS should travel to the next station. A gap of the required traveling time between the falling edge of the first PL and the rising edge of the next PL should be considered to present a real logical scenario. Two binary variables called $f_{m,t}$ and $r_{m,t}$ are proposed in order to denote the fall and rise edge's timing of each PL.

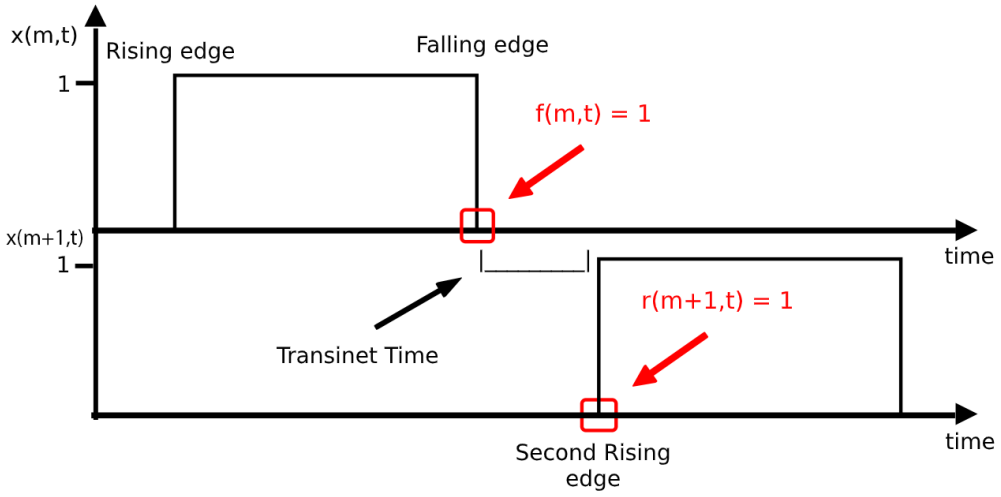


Figure 3.1 Capturing rising and falling edges of binary decision variable.

Equation (17) ensures that $f_{m,t} = 1$ only at the falling edge of $x_{m,t}$. The term $(x_{m,t} - x_{m,t-1})$ have three different possibilities, which are [-1, 0, and 1]. Constraint (3.17) guarantees that $f_{m,t} = 1$ if the value of $(x_{m,t} - x_{m,t-1})$ is [-1], which is the falling edge. Equation (3.18) ensures that $f_{m,t}$ should have a value of 1 at least once,

which is at the falling edge. At this stage, the falling edge timing in captured in $f_{m,t}$.

$$-1 \times f_{m,t} = f_{m,t} \times \left(x_{m,t} - x_{m,t-1}\right), \forall\, m, t \tag{3.17}$$

$$\sum_{t} f_{m,t} = 1\,, \forall\, m \tag{3.18}$$

In order to force the rising of the second PL (being available at the second station), the rising edge should take place after the falling edge of the previous station, considering the traveling and connecting/disconnecting time. This time is represented in the formulation as transient time (TT). Equations (3.19) and (3.20) ensure that $f_{m,t}$ and the next $r_{m,t}$ are separated by a time interval equals to TT as illustrated in Figure 3.1. At this stage, $r_{m,t} = 1$ after the previous falling edge timing plus the TT. The next step is to force the rising edge to take place at this captured time.

$$r_{m+1,t} = f_{m,t-TT}, \forall\, m\ where\ t > TT \tag{3.19}$$

$$\sum_{t} r_{m+1,t} = 0\,, \forall\, m\ where\ t < TT \tag{3.20}$$

The truck is considered to be available at the next station by forcing the rising edge to take place at the specified $t$ in $r_{m,t}$. This can be done using (3.21) that defines the rising time. Equation (3.22) ensures that only one rising edge can take place.

$$r_{m+1,t} = r_{m+1,t} \times \left(x_{m+1,t} - x_{m+1,t-1}\right), \forall\, m, t \tag{3.21}$$

$$\sum_{t} r_{m+1,t} = 1\,, \forall\, m \tag{3.22}$$

The MESS is considered to be a battery-based truck, equations (3.23) and (3.24) represent the state-of-charge of the battery inside the truck, as follows:

$$SOC_t^T = SOC_{t-1}^T + \Delta SOC_t^T \tag{3.23}$$

$$\Delta SOC_t^T = \frac{(P^{CH-T} - P^{DCH-T})\Delta T}{E^{MESS}} \tag{3.24}$$

where $SOC_t^T$ is the SOC of the MESS battery at time $t$; $\Delta SOC_t^T$ is the change in the SOC due to charging, discharging, and traveling; $P^{CH-T}$ and $P^{DCH-T}$ are the maximum charging and discharging rates, respectively; $E^{MESS}$ is the battery capacity in kWh.

**3.1.4 Decision variables constraints.** All decision variables constraints are mentioned in (3.25) - (3.27), where MDOD is the maximum depth of discharge for each battery.

$$P_{n,t}^{EV}, P_{i,t}^{EV-Total} \geq 0 \,, \forall\, n, i, t \tag{3.25}$$

$$(1 - MDOD) \leq SOC_{n,t}, SOC_t^T \leq 1 \tag{3.26}$$

$$x_{m,t}, y_{m,t}, f_{m,t} \,, r_{m,t} \in \{0,1\}, \forall\, m, t \tag{3.27}$$

The previously mentioned set of constraints can be generalized to model any number of charging stations while taking the computational time and problem complexity into consideration.

## 3.2. Case Studies

The case study is modeled as mixed-integer-nonlinear programming (MINLP) problem in order to highlight its effectiveness and the possible contribution to the system. Simulation is conducted on the known IEEE-38 bus system, which can be seen in Figure 3.2.

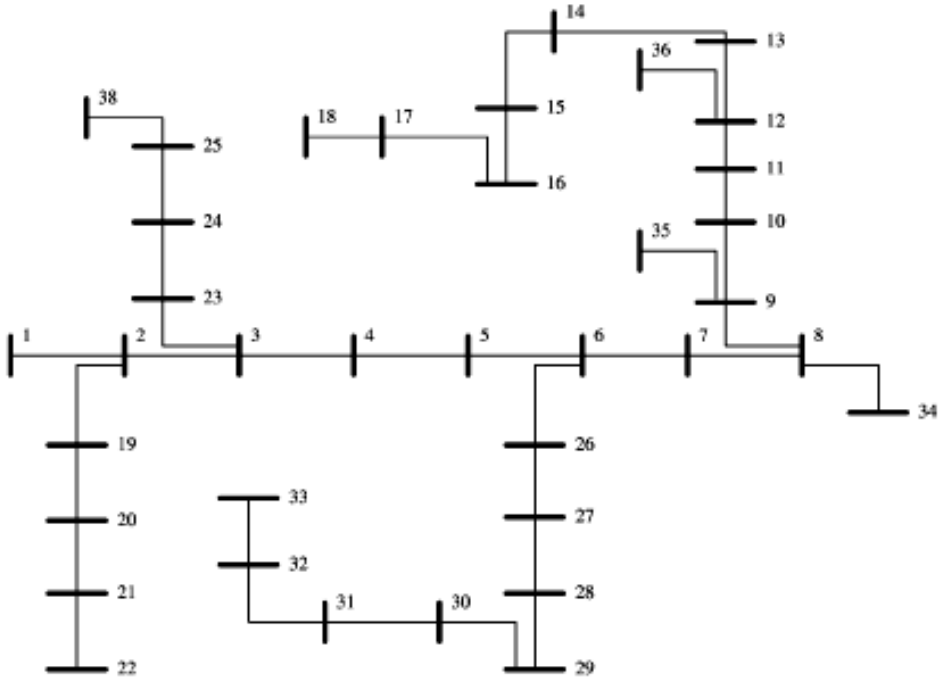


Figure 3.2 IEEE-38 bus system under study.

The system contains 38 buses represented as a set $i = \{1,2,3,\ldots,38\}$. Each EV is assumed to visit the PL once a day and the required energy for each car is provided the day ahead. The maximum battery capacity is made to be 40 kWh just for simplicity

but it might be different for each EV. Each EV may require less than or up to this value. Three different PLs are examined in the study with the specification illustrated in Table 3.1. The first PL is supplied from bus 9, while the second and third PLs are loaded on buses 18 and 36, respectively. The TT between each PL is calculated offline based on the distance between the buses and average truck speed. These values are in hours and it represents the traveling time, connecting, and disconnecting time. Figure 3.3 represents the variant grid price over the day [57].

Table 3.1 Problem parameters.

| **PLs specifications** | |
|---|---|
| EVs battery cap. | 40 kWh |
| Maximum charging rate | 9.6 kW |
| Maximum depth of discharge | 80% |
| Chargers Available in PL1 | 121 |
| Chargers Available in PL2 | 144 |
| Chargers Available in PL3 | 168 |
| Maximum discharge rate of MESS | 200 kW |
| Total batteries capacity | 4 MWh |
| TT between PL1 and PL2 | 1 hour |
| TT between PL2 and PL3 | 1 hour |
| TT between PL1 and PL3 | 2 hours |

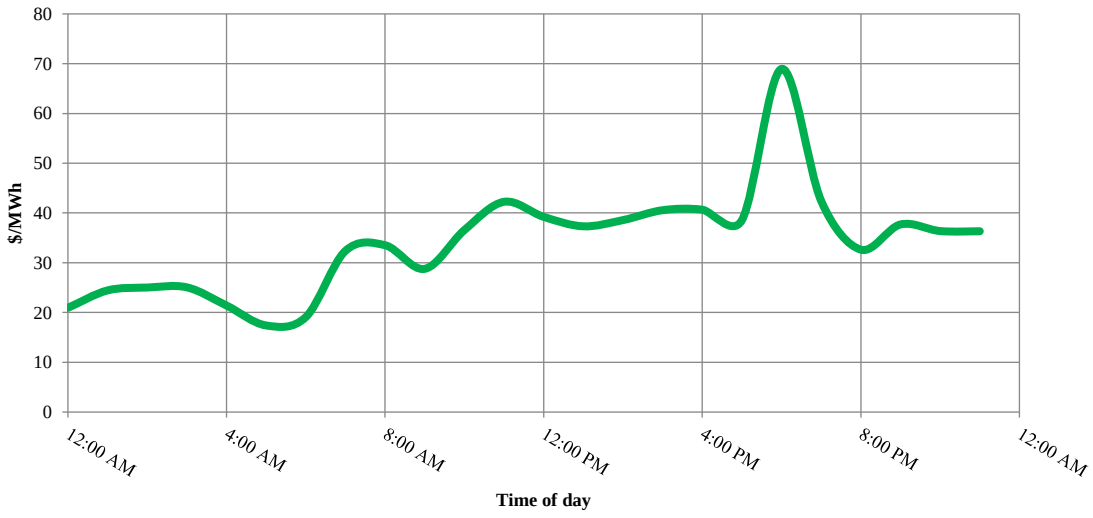


Figure 3.3 Grid price per hour for one day.

**3.2.1 Case study 1.** Case Study 1 represents the EVs demand from each PL without the integration of the MESS. Charging is uncontrolled and once the car is available at the station it starts charging (i.e., First-Come-First-Serve basis).

As shown in Figure 3.4, the total power demand of each PL is presented, noting that different peaks at different times take place in this scenario. PL1 reports a peak load of 1.12 MW at 4:00 AM, PL2 has a peak load of 0.9 at 5:00 PM, and PL3 has 1 MW at 10:00 AM.

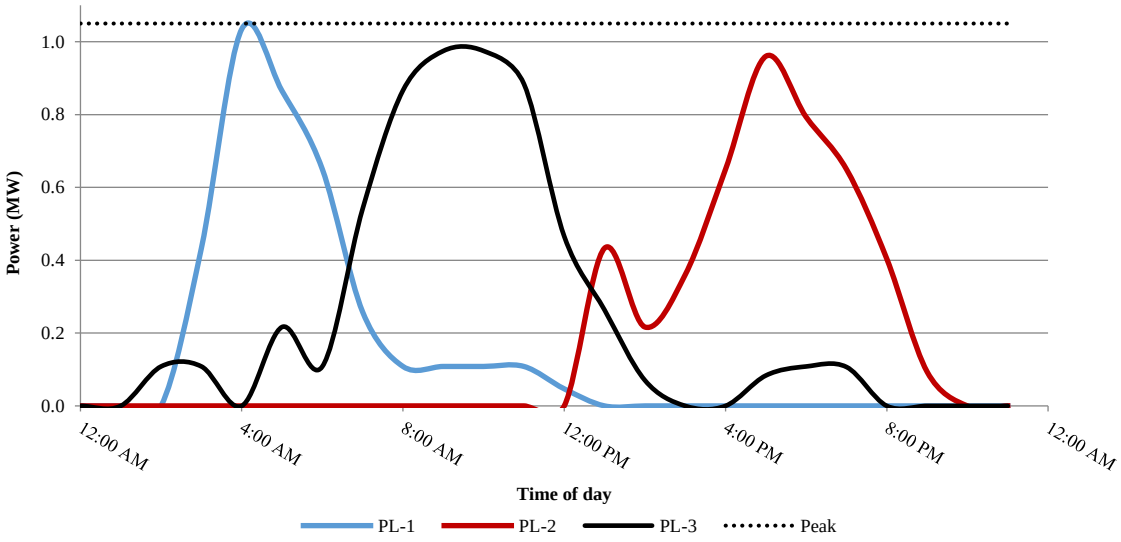


Figure 3.4 Power demand of each PL.

**3.2.2 Case study 2.** The MESS is dispatched in order to serve the associated PLs. It is expected to visit PL1, followed by PL3 and then PL2 at the end, according to the peak times as per Figure 3.4 in case 1.

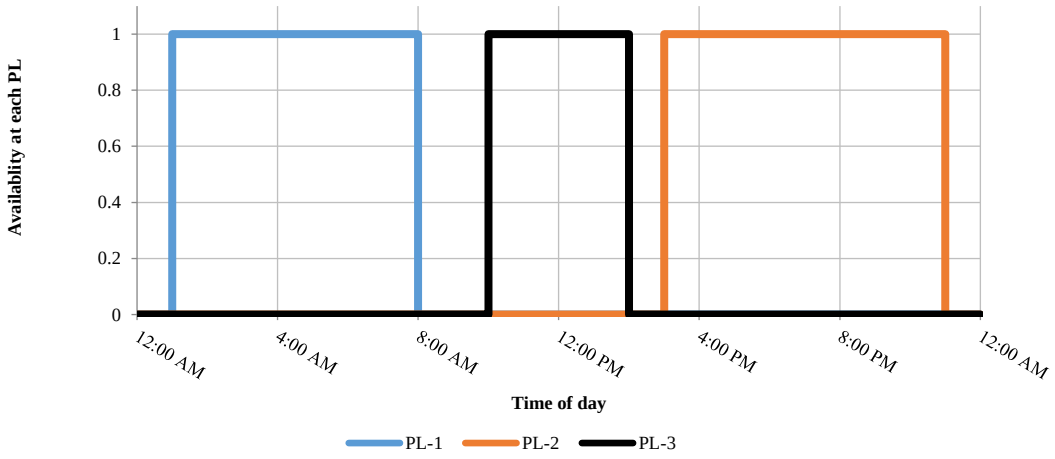


Figure 3.5 Availability of MESS at each PL.

Figure 3.5 shows the availability of the truck at each PL as well as the traveling time, which is mentioned between each PL in Table 1, i.e., one means MESS is available at PL. The expected visiting order takes place which proves the functionality of the proposed approach. The MESS is available in PL1 from 11:00 AM until 8:00 AM, then traveling to PL3 which will take 2 hours and will stay at PL3 until 1:00 PM. At the end, it arrives PL2 at 2:00 PM and stays until 11:00 PM.

The power drained from the system by each charging station after the visit of the MESS is presented in Figure 3.6, which is, overall, less than the power consumed in the first case study. The discharging rate vs time at each PL is illustrated in Figure 3.7, it decides to discharge with maximum discharging rate since the demand is high and there is available energy in the MESS's battery, i.e., considering the maximum depth-of-charge. Finally, Figure 3.8 represents the state-of-charge (SOC) of the battery, noting that at the end of the day, 20% of the battery is maintained which achieves the MDOD limit.

A summary of the total cost of all case studies is shown in Table 3.2. It turned out that, in case 1, the energy costs for PL1, PL2, and PL3 are $85.9157, $201.512, and $204.88, respectively, resulting in a total energy cost of $492.30. On the other hand, case 2 reports $62.84, $149.86, and $166.13 for PL1, PL2, and PL3, respectively, with a total energy cost of $378.847 and total savings up to 23% as illustrated in Table 3.2.

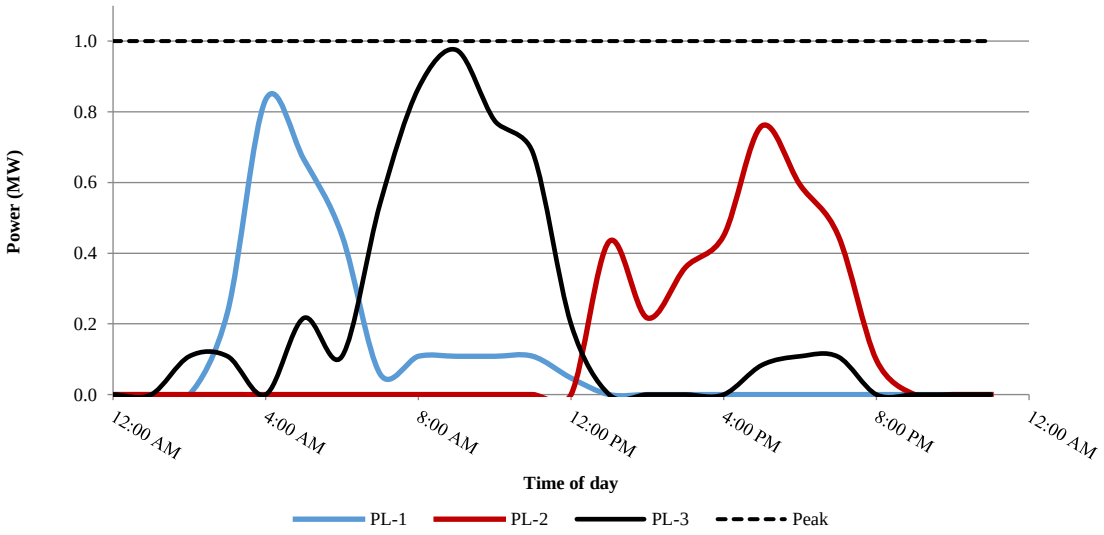


Figure 3.6 Power demand of each PL after mobile storage visit.

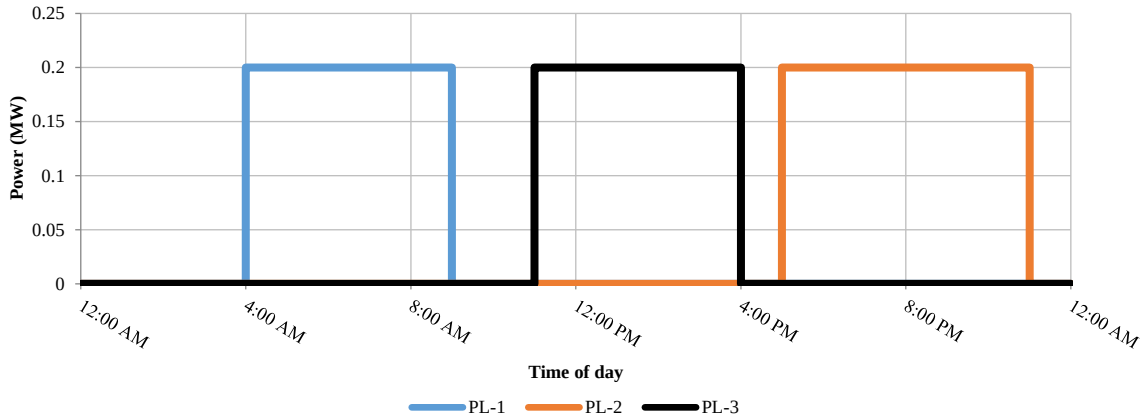


Figure 3.7 Case 2 - MESS discharging rate.

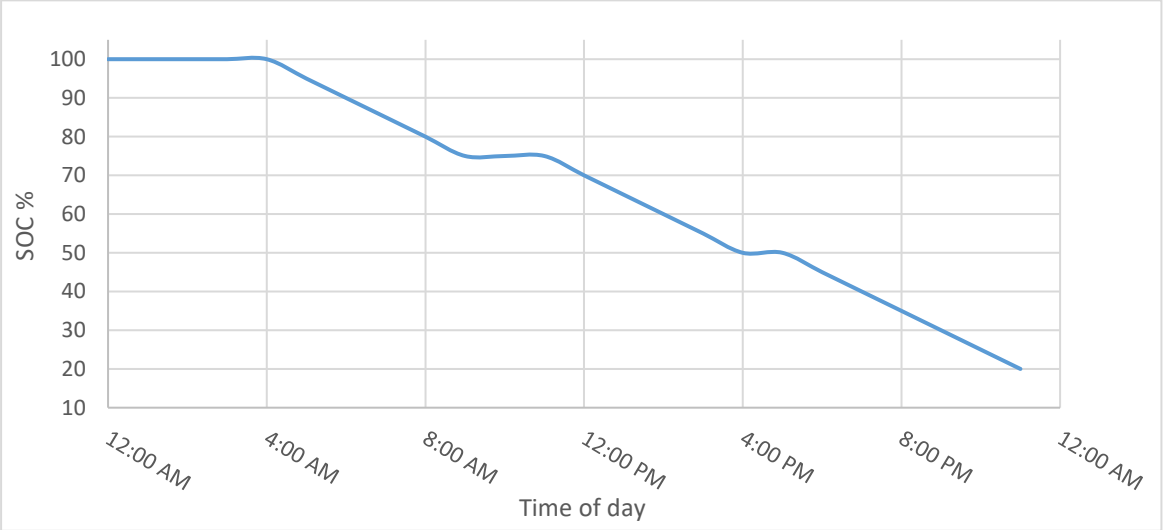


Figure 3.8 MESS results: battery SOC.

Table 3.2 Summary of simulation results.

| | Case 1 | Case 2 |
|---|---|---|
| Energy cost PL1 | $85.9157 | $62.847 |
| Energy cost PL2 | $201.512 | $149.869 |
| Energy cost PL3 | $204.88 | $166.13 |
| Total energy cost | $492.308 | $378.847 |
| Savings | - | 23.04% |

**3.3. Conclusion.** Distribution networks will face many challenges owing to the rapid increase of EVs in the market and the increasing load demand to charge these EVs. Due to the uncertainty of these loads, many technical issues will arise such as congestion on the distribution side and voltage drops. The technology of storage systems is gaining a lot of attention and has been the focus of rigorous study. This paper proposes a scheduling algorithm for an MESS to address the increased demand of charging stations within a specific area. Two case studies were discussed to illustrate the contribution of the proposed algorithm. The proposed algorithm has successfully reduced the total operational cost of each one of the 3 PLs associated in the case study as shown by the reduction in the aforementioned costs of 23% in the simulation results. Additionally, if demand exceeds the generation limit, excess energy is required to fulfill that unmet demand which is readily supplied using MESS; whereas there would not be any avenue of supplying it without the proposed system.

## Chapter 4. Optimal Dispatch of a Mobile Storage Unit to Support EV Charging Stations

In this chapter, an MESS owned by and serves multiple utilities sharing the same geographical area in order to shave the peak demand and minimize the operational cost is conducted. The proposed system will dynamically dispatch the MESS to serve the associated PLs during the day in which these PLs will coordinate arrival EVs charging behavior to have the peak load at the time that the MESS is available at this particular PL. As shown in Figure 4.1, the algorithm has the choice to determine the order of visiting the PLs based on its coordinated load demand while satisfying all EVs requirements. The departure and arrival time between the PLs are separated by a gap called Transient Time (TT) which represents the traveling time considering the traffic, the speed of the MESS, connecting, and disconnecting time from the power system. The following section will contain a discussion about the problem formulation of day-ahead scheduling of MESS to serve the requirements of different charging stations contributing with different percentages to the MESS's capital cost.

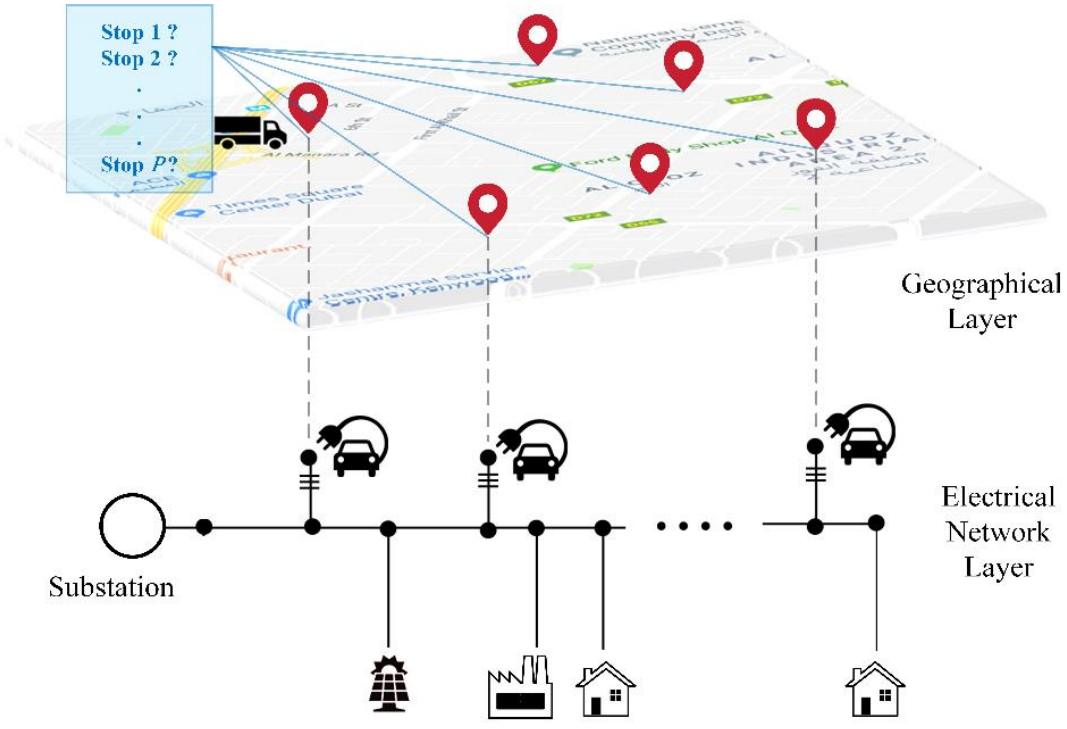


Figure 4.1 Overall mapping scheme illustrating the overlaying of the geographical and electrical layers.

## 4.1. Problem Formulation

Different models are integrated into the problem formulation in order to implement the proposed system, as depicted in Figure 4.2. The power flow model relates the line current, bus voltage, and power losses to the MESS power and location, while the MESS model represents the dynamicity in selecting the sequence of visiting the PLs.

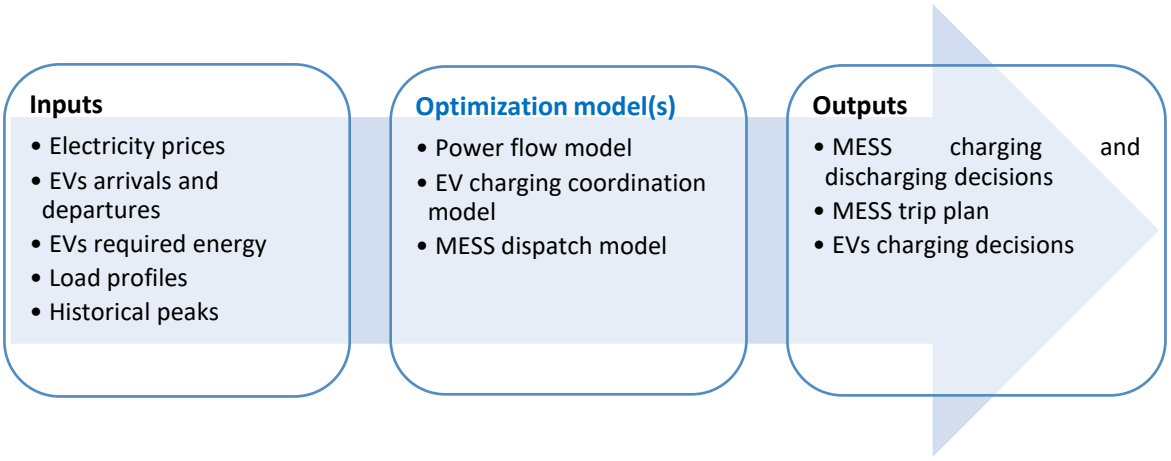


Figure 4.2 Proposed model structure.

The objective function shown in (4.1) aims to minimize the total cost of the total drained power by the PLs to charge the arrival EVs and the total demand charges. As shown in (4.2), the historical peak demand $P_i^{MAX-Target}$ is used to calculate the demand charges, the extra peak demand charges are only considered for the power exceeds the $P_i^{MAX-Target}$. The additional demand charges $C^{peak}$ will be considered to be zero if the peak is not exceeding the historical peak demand, as follows:

$$\min \sum_{i \in \mathbb{I}_{ev}} \left( \sum_{t \in \mathbb{T}} \left( C_t^{grid} P_{i,t}^{ev} \Delta t \right) + C_i^{peak} \right) \tag{4.1}$$

$$C_i^{peak} = \begin{cases} 0 & , \forall \left( P_i^{ev-MAX} - P_i^{MAX-Target} \right) \leq 0 \\ C^{kw} \left( P_i^{ev-MAX} - P_i^{MAX-Target} \right) & , otherwise \end{cases} , \forall i \in \mathbb{I}_{ev} \tag{4.2}$$

where $C_t^{grid}$ refers to the variable grid cost at each time interval; $P_{i,t}^{ev}$ is the total power consumed by EVs at each bus and each time interval; $\mathbb{T}$ is the set of all the time segments; $\mathbb{I}_{ev}$ is a subset of buses loaded by a PL; $C_i^{peak}$ is the total extra peak demand charges for charging stations on bus $i$; $C^{kw}$ is the demand charges in \$/kW; $P_i^{ev-MAX}$ is

the peak demand of the charging stations on bus $i$; $P_i^{MAX-Target}$ is the historical recorded or targeted recorded peak demand.

**4.1.1 Power flow linearized constraints.** The nonlinear power balance equations are presented in (4.3) and (4.4). The active power consumption at any bus $\boldsymbol{i}$ consists of the residential, commercial, and industrial customers, in addition to, the EV charging stations are articulated and defined in (4.5). The generated power at any bus $\boldsymbol{i}$ is the sum of the generated power from the DG units and the power consumed from the grid is given by (4.6):

$$P_{i,t}^{G} - P_{i,t}^{L} = \sum_{j \in \mathbb{I}} V_{i,t}\, V_{j,t}\left(G_{i,j}\, cos\, \delta_{i,j} + B_{i,j}\, sin\, \delta_i\right)\ , \forall i, t \tag{4.3}$$

$$Q_{i,t}^{G} - Q_{i,t}^{L} = \sum_{j \in \mathbb{I}} V_{i,t}\, V_{j,t}\left(G_{i,j} \cos \delta_{i,j} + B_{i,j} \sin \delta_i\right), \forall i, t \tag{4.4}$$

$$\left.\begin{aligned} P_{i,t}^{L} = P_{i,t}^{L-R} + P_{i,t}^{L-C} + P_{i,t}^{L-I} + P_{i,t}^{L-EV} \quad \forall i, t \\ P_{i,t}^{L-R} = 0 \;\forall\; i \notin \mathbb{I}_{res} \\ P_{i,t}^{L-C} = 0 \;\forall\; i \notin \mathbb{I}_{com} \\ P_{i,t}^{L-I} = 0 \;\forall\; i \notin \mathbb{I}_{ind} \\ P_{i,t}^{L-EV} = 0 \;\forall\; i \notin \mathbb{I}_{ev} \end{aligned}\right\} \tag{4.5}$$

$$\left.\begin{aligned} P_{i,t}^{G} = P_{i,t}^{Grid} + P_{i,t}^{DG} \\ Q_{i,t}^{G} = Q_{i,t}^{Grid} + Q_{i,t}^{DG} \end{aligned}\right\} \tag{4.6}$$

where $i$ and $j$ denote bus indices; $\mathbb{I}$ is the set of all system buses; $P_{i,t}^{L}$ and $Q_{i,t}^{L}$ represent real and reactive powers consumed at bus $i$ and time $t$, respectively; $P_{i,t}^{G}$ and $Q_{i,t}^{G}$ are the real and reactive generated powers in p.u., respectively; $G_{i,j}$ and $B_{i,j}$ represent real and imaginary components of the $i-j$ element in the Y-bus matrix; $V_{i,t}$ and $\delta_i$ represent the voltage magnitude in p.u. and angle, respectively; $\mathbb{I}_{res}$, $\mathbb{I}_{com}$, $\mathbb{I}_{ind}$, and $\mathbb{I}_{ev} \subset \mathbb{I}$ are the subsets of the residential customers, commercial customers, industrial customers, and EV parking lots buses respectively; $P_{i,t}^{L-R}$ is the power of the residential load and it is zero for all non-residential buses. Similarly, $P_{i,t}^{L-C}$, $P_{i,t}^{L-I}$, and $P_{i,t}^{L-EV}$ are the commercial, industrial, and EV parking lots power; $P_{i,t}^{Grid}$ and $Q_{i,t}^{Grid}$ are the real and reactive injected powers from the grid, respectively; $P_{i,t}^{DG}$ and $Q_{i,t}^{DG}$ are the real and reactive injected powers from the DG units, respectively.

The linear power flow model proposed in [47] is used to reduce complexity and

save computational time. The linearized equations are provided in (4.7) and (4.8).

$$(P_{i,t}^{L} - P_{i,t}^{G})\, V_{i,t} + \; 2P_{i,t}^{G} - 2P_{i,t}^{L} = \sum_{j \in \mathbb{I}} \left(V_{j,t} G_{i,j} + B_{i,j} \delta_j\right) \tag{4.7}$$

$$(Q_{i,t}^{L} - Q_{i,t}^{G})\, V_{i,t} + \; 2Q_{i,t}^{G} - 2Q_{i,t}^{L} = -\sum_{j \in \mathbb{I}} \left(V_{j,t} B_{i,j} + G_{i,j} \delta_j\right) \tag{4.8}$$

The voltage levels have to be maintained within acceptable limits as expressed in (4.9). Also, the thermal line limits impose an upper limit on the line current magnitude as in (4.10):

$$V^{min} \leq \; V_{i,t} \; \leq V^{max} \qquad \forall\, i, t \tag{4.9}$$

$$I_{i,j,t} \; \leq \; I_{i,j}^{max} \tag{4.10}$$

where $V^{min}$ and $V^{max}$ are the minimum and maximum permissible voltage levels in p.u., respectively; $I_{i,j}^{max}$ and $I_{i,j,t}$ is the maximum allowable current and the actual current at time $t$ through the line between buses $i$ and $j$, respectively.

**4.1.2 EV charging constraints.** Equation (4.11) describes the total power for each charging station. The first term in (4.11) is the required EVs charging power; the second term is the power injected from the MESS to each PL. Charging decisions are restricted by the availability of the EV and it can take a value from zero up to the full charging rate as in (4.12), as follows:

$$P_{i,t}^{L-EV} = \left( \sum_{v \in \mathbb{V}_i} \frac{X_{v,i,t}^{EV}\, P_v^{CH}}{\eta_{ch}\, S^{base}} \right) - P_{i,t}^{MS}, \forall i \in \mathbb{I}_{ev}, t \tag{4.11}$$

$$\begin{aligned} X_{v,i,t}^{EV} &\leq A_{v,i,t}\,, \forall v, i, t \\ 0 \leq X_{v,i,t}^{EV} &\leq 1, \forall v, i, t \end{aligned} \tag{4.12}$$

where $v$ and $\mathbb{V}_i$ are the index and the subset of chargers on bus $i$, respectively; $X_{v,i,t}^{EV}$ is the charging decision as a fraction of the charger capacity; $P_v^{CH}$ is the charger capacity in kW; $\eta_{ch}$ is the efficiency of charging; $S^{base}$ is the system base power in kVA for the per-unit system; $A_{v,i,t}$ is a binary parameter indicating whether charger $v$ on bus $i$ is occupied with an EV at time $t$, i.e. if $A_{v,i,t} = 1$, then an EV is plugged into the charger; $P_{i,t}^{MS}$is the power injected from the MESS.

The state of charge (SOC) of each EV is updated with the charging energy as in

(4.13) and (4.14). Equation (4.15) is used to ensure satisfying the pre-required demand for each EV.

$$SOC_{v,i,t}^{EV} = SOC_{v,i,t-1}^{EV} + \Delta SOC_{v,i,t}^{EV} \tag{4.13}$$

$$\Delta SOC_{v,i,t}^{EV} = \frac{X_{v,i,t}^{EV} P_v^{CH-EV} \Delta T}{E_{v,i}^{BAT}} \tag{4.14}$$

$$SOC_{v,i,t}^{EV} \leq SOC_{v,i}^{REQ} \tag{4.15}$$

where $SOC_{v,i,t}^{EV}$is the SOC at time $t$ for each EV; $\Delta SOC_{v,i,t}^{EV}$ the change in the SOC due to charging; $\Delta T$ is the time segments in hours; $E_{v,i}^{BAT}$ is the battery capacity in kWh; $SOC_{v,i}^{REQ}$is the required SOC by each EV driver.

**4.1.3 MESS modeling.** The trip plan of the MESS is exed in the next subsection in sequencing and scheduling modeling. Besides the trip plan, when the MESS is in transit or at any parking lot, the SOC of the MESS battery at each time segment is updated as in (4.16) and (4.17). It is affected by the injected energy and the MESS traveling consumption, as follows:

$$SOC_t^{MS} = SOC_{t-1}^{MS} + \Delta SOC_t^{MS} \tag{4.16}$$

$$\Delta SOC_t^{MS} = \frac{(X_t^{C-MS} P^{CH-MS} - X_t^{DCH-MS} P^{DCH-MS} - P_t^{M-MS})\Delta T}{E^{MESS}} \tag{4.17}$$

Equation (4.18) maintains the battery limits, as follows:

$$SOC^{MS-MIN} \leq SOC_t^{MS} \leq 1.0 \tag{4.18}$$

where $SOC_t^{MS}$ is the SOC of the MESS battery at time $t$; $\Delta SOC_t^{MS}$ is the change in the SOC due to charging, discharging, and traveling; $X_t^{C-MS}$ and $X_t^{DCH-MS}$ are the charging and discharging decision variables, respectively; $P^{CH-MS}$ and $P^{DCH-MS}$ are the maximum charging and discharging rates, respectively; $P_t^{M-MS}$ is the power consumed due to traveling between PLs; $E^{MESS}$ is the battery capacity in kWh; $SOC^{MS-MIN}$is the minimum SOC of the MESS.

The MESS is owned by different PLs contributing with different percentages to the capital cost of the MESS. According to this contribution, each PL should get an amount of the energy equivalent to its share as in (4.19), as follows:

$$\sum_{t \in \mathbb{T}} P_{i,t}^{MS} \Delta T = \gamma_i \sum_{i \in \mathbb{I}_{ev}} \left( \sum_{t \in \mathbb{T}} P_{i,t}^{MS} \Delta T \right), i \in \mathbb{I}_{ev} \tag{4.19}$$

$$\sum_{i \in \mathbb{I}_{ev}} \gamma_i = 1$$

where $\gamma_i$ is the per-unit sharing of each charging station.

**4.1.4 Scheduling and sequencing modeling.** The overall integrated scheduling and sequencing approach relies on decoupling the temporal and spatial elements of the problem. This is done by optimizing the durations of the visits. Then, the assignment of the PLs to the visiting order 1, 2, 3, …, $\boldsymbol{N_P}$ as explained in Section 4.1 and shown in Figure 4.1 is carried out. Thus, the first part that manages the duration of the MESS visits assumes a fixed order using the binary decision variable $\boldsymbol{X_{p,t}}$, where $\boldsymbol{X_{p,t} = 1}$ indicates that the MESS is connected to parking lot $\boldsymbol{p}$ at time $\boldsymbol{t}$. A binary decision variable $\boldsymbol{M_{p,t}}$ is introduced to express the traveling phase between parking lots $\boldsymbol{p}$ and $\boldsymbol{p + 1}$. At any time segment, the MESS can be either connected to a parking lot $\boldsymbol{p}$ or traveling between two PLs as in (4.20). The MESS should visit all the PLs as in (4.21) and it should also travel from all PLs except the last one as in (4.22). If the MESS leaves a parking lot, it cannot return to it again, as in (4.23). The constraint in (4.24) ensures that the MESS can be connected to parking lot $\boldsymbol{p}$ only if it was connected to another parking lot 1, 2, …, $\boldsymbol{p - 1}$ or the same parking lot $\boldsymbol{p}$ at time $\boldsymbol{t - 1}$ and the same holds for the traveling between the parking lots as in (4.25). Equations (4.26) and (4.27) ensure that a traveling phase takes place after visiting $\boldsymbol{p}$ and before arriving at $\boldsymbol{p + 1}$.

$$\sum_{p \in \mathbb{P}} X_{p,t} + M_{p,t} = 1 \; \forall t \tag{4.20}$$

$$\sum_{t \in \mathbb{T}} X_{p,t} \geq 1 \; \forall p \tag{4.21}$$

$$\sum_{t \in \mathbb{T}} M_{p,t} \geq 1 \;\; \forall p = \{1,2, \dots, N_p - 1\} \tag{4.22}$$

$$X_{p,t} \leq X_{p,t-1} \;\; \forall \, p, t \tag{4.23}$$

$$X_{p,t} \leq \sum_{p=1}^{p} X_{p,t-1} \;\; \forall p, t \tag{4.24}$$

$$M_{p,t} \leq \sum_{p=1}^{p} M_{p,t-1} \ \forall p,t \tag{4.25}$$

$$X_{p,t} - \ M_{p,t+1} \leq 1 \quad \forall p = \{1,2,\dots,N_p - 1\}, t \tag{4.26}$$

$$M_{p,t} - \ X_{p+1,t+1} \leq 1 \ \forall p = \{2,\dots,N_p\}, t \tag{4.27}$$

where $X_{p,t}$ is a binary variable indicating if the MESS is available at PL $p$ and $M_{p,t}$ is a binary variable indicating if the MESS is traveling between PLs.

The second part of the proposed sequencing and scheduling formulation is to decide the optimal sequence of visiting the actual PLs. Thus, another binary variable is introduced $D_{i,p}$, where $D_{i,p} = 0 \ \forall i \notin \mathbb{I}_{ev}$. For example, if $D_{9,2}$ = 1, this means that the parking lot on bus $i = 9$ will be the second parking lot, i.e., $p = 2$, to be visited by the MESS. Each parking lot should be visited once as in (4.28) and each visit should be assigned one parking lot as in (4.29). The constraint in (4.30) ensures that the MESS can inject power at bus $i$ only if it is connected to the parking lot assigned to this bus. The power consumption during the traveling phase of the MESS is modeled by (4.31) taking into consideration the distance $S_{i,j}$ between locations at buses $i$ and $j$ where $i \neq j$ and the power consumption rate per km.

$$\sum_{i \in \mathbb{I}_{ev}} D_{i,p} = 1 \tag{4.28}$$

$$\sum_{p \in \mathbb{P}} D_{i,p} = 1 \tag{4.29}$$

$$P_{i,t}^{MS} = D_{i,p} \, X_{p,t} ( \, X_t^{DCH-MS} P^{DCH-MS} - X_t^{C-MS} \, P^{CH-MS}) \quad \forall \, i,t \tag{4.30}$$

$$P_t^{M-MS} = \sum_{i \in \mathbb{I}_{ev}} \sum_{j \in \mathbb{I}_{ev}} \sum_{p \in \mathbb{P}} \frac{M_{p,t} D_{i,p} \, D_{j,p+1} \, S_{i,j} \, \rho}{\Delta T} \tag{4.31}$$

where $D_{i,p}$ is the binary variable that assigns each PL location to the optimal visiting order; $S_{i,j}$ is the distance between two locations; $\rho$ is the consumption rate in kWh/km.

**4.1.5 Decision variables constraints.** In this section, the variables constraints are illustrated as shown:

$$P_v^{CH}, \ P^{DCH-MS}, \ P^{CH-MS}, P_t^{M-MS}, \geq 0 \qquad \forall \, t \tag{4.32}$$

$$(100 - MDOD) \leq SOC_t^{MS}, SOC_{v,i,t}^{EV} \leq 100 \qquad \forall\ t \qquad (4.33)$$

$$X_t^{C-MS}, X_t^{DCH-MS},\ X_{v,i,t}^{EV}, X_{p,t}, M_{p,t}, D_{i,p} \in \{0,1\} \qquad \forall\ i,p,t,v \qquad (4.34)$$

where MDOD is the Maximum depth of charge that maintains longer battery life.

The previously mentioned set of constraints can be generalized to model any number of PLs.

### 4.2. Simulations and Results

To validate the proposed system, a mixed-integer nonlinear programming (MINLP) problem is modeled to highlight the contribution of the MESS. The simulations are conducted on a 36-bus real radial feeder located in Ontario, Canada [48] shown in Figure 4.3. This distribution system is rated at 16.185 MVA, a medium voltage of 16 kV, and extends for 30 kilometers. Line's impedance and lengths are given in [48]. The daily load profiles, which are obtained for typical loads on a winter day [49], are broken into three categories. Industrial load on bus 4, commercial load on buses 7 and 36, and residential load on the remaining buses. The different daily load profiles can be seen in Figure 4.4 while the grid energy price [57] is shown in Figure 4.5. To solve the optimization problem, the General Algebraic Modeling Software (GAMS) is used, which is a powerful, effective, and simple platform for power system optimization [50]. For the proposed approach, the BARON solver is used, which implements the branch-and-bound type of global optimization algorithms to guarantee the global optimal.

The time horizon is divided into 24-time slots per day, each time slot is one hour span and represented as a set t = {1, 2, 3, ..., 24}. The system contains 36 buses represented as a set i = {1, 2, 3, ..., 36}. The assumption of each EV is coming to the PL once a day is made. The required energy for each EV is provided a day ahead and it should be delivered during the EV available time at the PL. The maximum battery capacity of each EV is assumed to be 90 kWh but it might be different for each EV. Each EV may request to get less than or up to this value. Three different PLs are examined in this study, the specifications of which are provided in Table 4.1. PL1 is supplied from bus 9, while PL2 and PL3 are loaded on buses 18 and 36, respectively. Several case studies are presented to investigate the effect of the proposed approach. The first case study is conducted on the PLs under an FCFS basis, where the charging requests are processed and executed by the order of their arrival, i.e., charging starts

once the EV is available at the PL. The second case study demonstrates the effect of EVs coordination on shaving the peak demand. The third case study focuses on the impact of integrating the MESS model. In all case studies presented, arbitrary historical peak demand for each PL to be 0.7, 0.8, 1 MW for PL1, PL2, and PL3, respectively, are assumed.

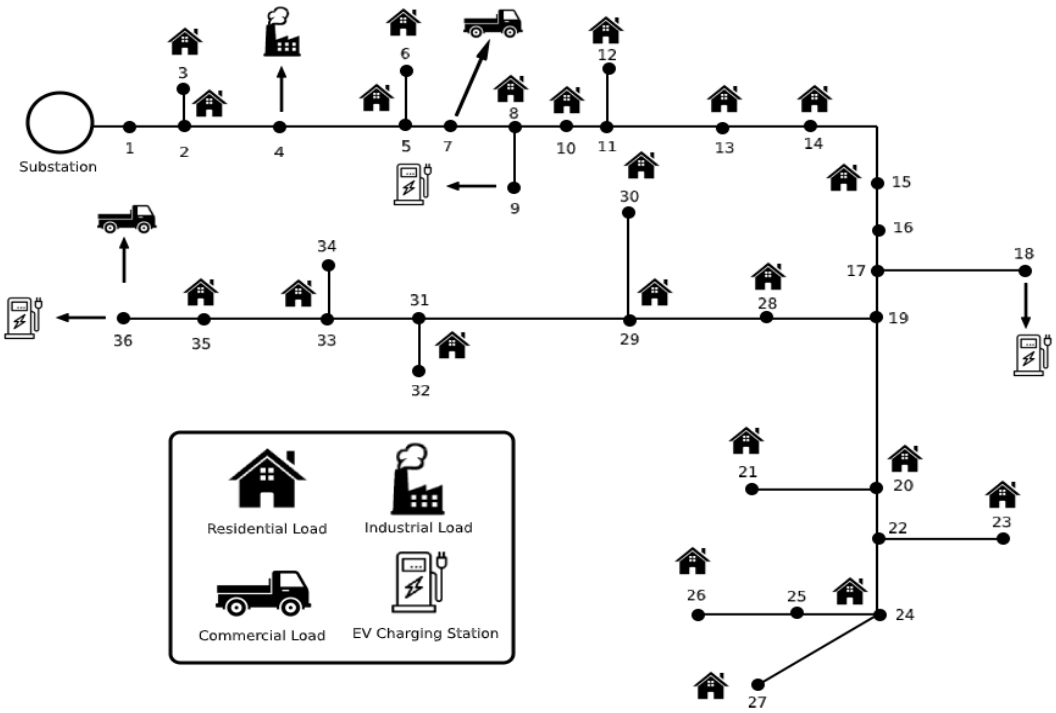


Figure 4.3 Radial system under study.

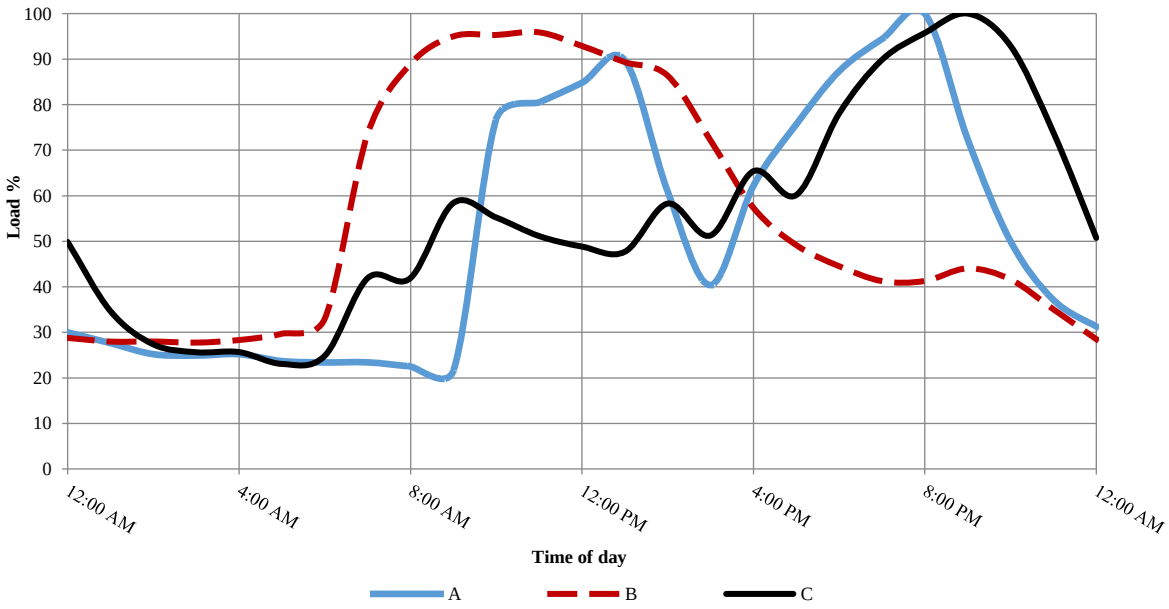


Figure 4.4 Different load profiles: A) Residential, B) Commercial, C) Industrial.

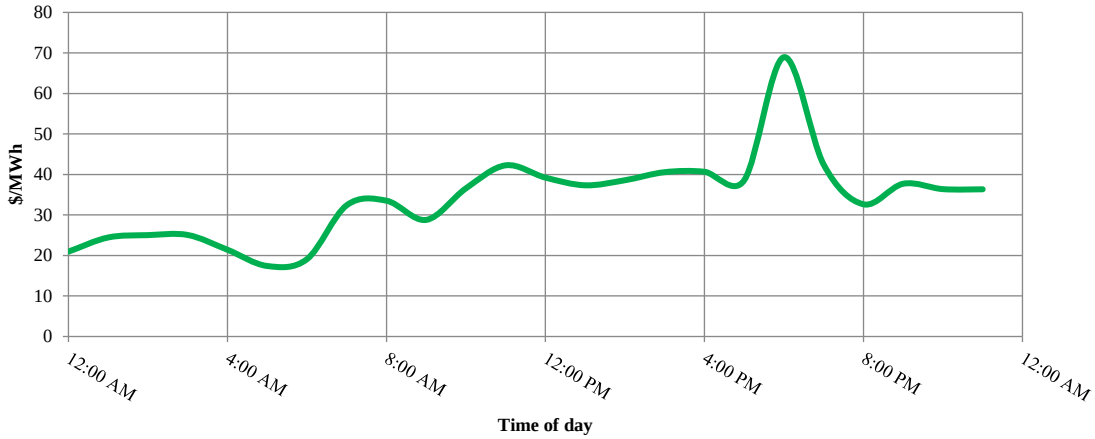


Figure 4.5 Grid price per hour for one day.

Table 4.1 Simulation parameters.

| | PL-1 | PL-2 | PL-3 |
|---|---|---|---|
| Chargers available | 50 | 50 | 75 |
| Maximum charging rate | 22 kW | 22 kW | 22 kW |
| Historical peak demand | 0.7 MW | 0.8 MW | 1 MW |
| Peak demand charge | $9.1/kW | | |

**4.2.1 Case 1: FCFS without MESS.** In this case, we apply FCFS, where the EVs start to charge once they are plugged in until the delivery of required energy is done as described in [51]. Figure 4.6 presents the power consumed by each parking lot and the historical peak for each one.

Three different peaks during different time segments took place. As shown in Figure 4.6, PL1 has a peak load of 0.93 MW at 2:00 PM and 3:00 PM, PL2 has 1.1 MW peak load at 7:00 AM and 8:00 AM and PL3 has 1.43 MW at 4:00 PM and 5:00 PM. All of them exceeds the $P_i^{MAX-Hist}$, by 32.2%, 37.5%, and 43%, respectively. This situation results in an extra demand charge of $2,138.5, $2,730, and $3,913 for PL1, PL2, and PL3, respectively, in addition to the charging cost. In the absence of the coordination and the MESS integration, the total extra demand charges are found to be $8,781.5 for the three PLs at the end of the day. In addition to the historical peak cost which is $22,750, the total encountered cost is found to be $31,979 as shown in Table 4.3.

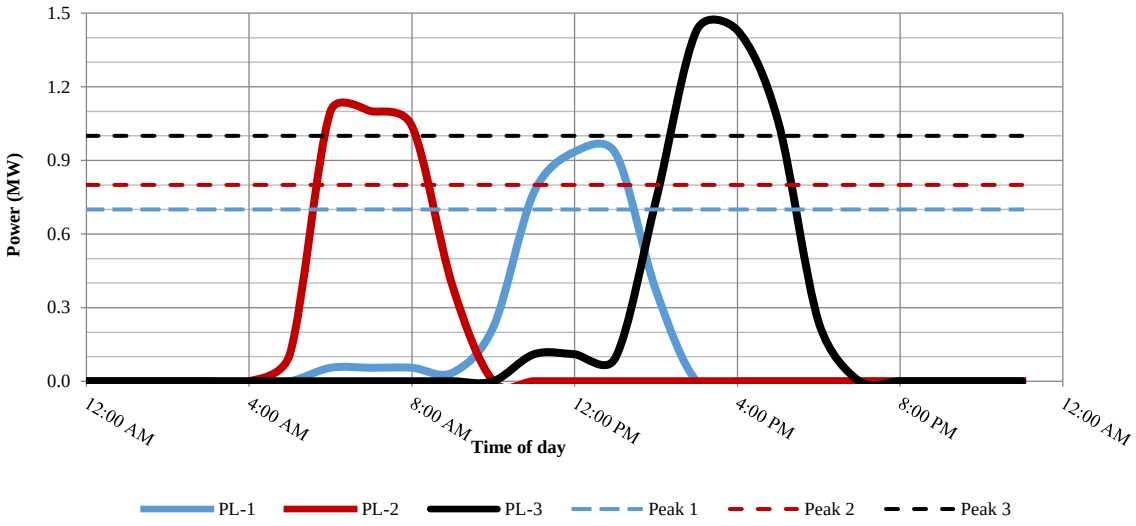


Figure 4.6 Case 1 - Power consumed by each PL under FCFS scheme.

**4.2.2 Case 2: EV coordinated charging without MESS.** The coordination constraints are applied in case 2. EVs charging is optimized to ensure minimum total cost taking into consideration the charging cost and demand charges, the proposed approach coordinates the charging behavior to avoid higher peak value and to charge the EVs in the lowest price time if possible, considering the availability time of the EVs. Figure 4.7 shows the power consumed by each PL. Each PL has its historical or targeted peak demand, on which the peak demand charges are billed, as explained in the formulation.

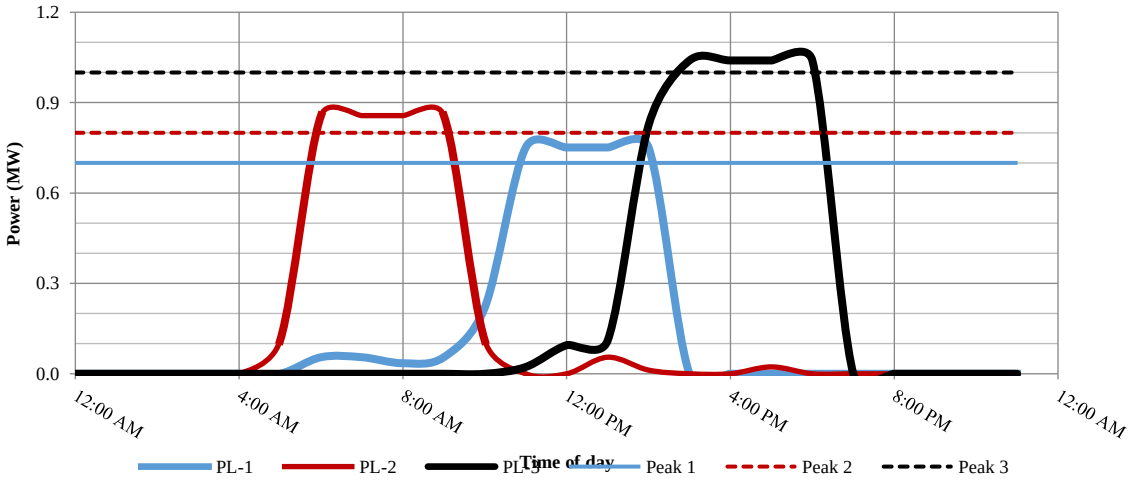


Figure 4.7 Case 2 - PLs power consumption with coordinated EV charging.

As shown in Figure 4.7, the proposed coordination scheme succeeds in shaving the power peaks; however, it did not entirely remove the extra demand charges. The

peak in PL1 is not exceeding the 0.75 MW limit during the period from 12:00 PM to 3:00 PM, which represents 7.14% (instead of 32.2% in the first case study) above the historical data and a demand charge of $466.37. This results in a reduction of 0.18 MW and a savings of $1,672.13 in PL1. PL2 and PL3 reported a peak load of 0.86 and 1.04 MW, which represent 7.5% and 4% (instead of the previously obtained 37.5% and 43%) above the $P_i^{MAX-Target}$ and result in an extra demand charge of $517.56 and $364 and a total demand charge of $7,797.56 and $9,464, respectively. The peak periods of PL2 and PL3 are taking place in the periods 7:00 AM and 4:00 PM till 10:00 AM and 7:00 PM, respectively. This leads to a reduction of 0.24 and 0.39 MW and savings of $2,212.44 and $3,549 for PL2 and PL3, respectively. The total demand charges are reduced; however, the energy consumption cost is increased since some EVs have been coordinated to charge at a relatively higher price time to minimize the demand charges. Energy consumption costs are $495.56 in comparison to the $447.97 in Case 1 (i.e., 10.9% increase). In the presence of EVs charging coordination, the total cost is found to be $24,573.49 for the three PLs. This is a reduction of 23.15% in the total cost from the previous case study.

**4.2.3 Case 3: EV coordinated charging with MESS.** In this case study, the MESS is dispatched. The Nikola One truck [52] is selected and used since it has a payload capacity of 29,500 kg. The truck is loaded with 47 batteries that weigh a total of 25,380 kg and has a capacity of 4 MWh, each battery weighs 540 kg and has a capacity of 85 kWh, as discussed in Table 4.2. The cost of the truck can be shared with different percentages among a group of PLs based on their needs. In this case study, an equal share between charging stations is assumed for simplicity. The energy delivered to each PL is equal to or less than 33% of the possible supplied energy. The minimum battery's SOC level is set to 20% to maintain a longer battery lifetime. And it is assumed to be 100% at the beginning of the day.

As illustrated in Figure 4.8, dispatching the MESS succeeds in mitigating the extra demand charges completely and supply power to the EVs if it is available at the PL. For PL1, the peak demand does not exceed the $P_i^{MAX-Target}$, which is 0.7 MW and it resulted in shifting the peak period from 1:00 PM to 3:00 PM instead of 12:00 PM to 3:00 PM. PL2 and PL3 did not exceed the $P_i^{MAX-Target}$ as well and maintained a peak

demand of 0.8 and 1 MW, respectively. This peak demand took place from 7:00 AM to 8:00 AM for PL2 and from 4:00 PM to 6:00 PM for PL3. For all PLs, the extra demand charges equal to zero since no $P_i^{MAX-Target}$ has been exceeded, while the historical demand charges are $22,750. The operation cost is found to be $99.78, $85.23, and $185.204 for PL1, PL2, and PL3, resulting in a total operation cost of $370.21 for all PLs at the end of the day.

Table 4.2 MESS specifications.

| **MESS specifications** | |
|---|---|
| Battery capacity | 85 kWh |
| Battery weight | 540 kg |
| Number of batteries | 47 |
| Total batteries weight | 25,380 kg |
| Truck payload capacity | 29,500 kg |
| Total batteries capacity | 4 MWh |

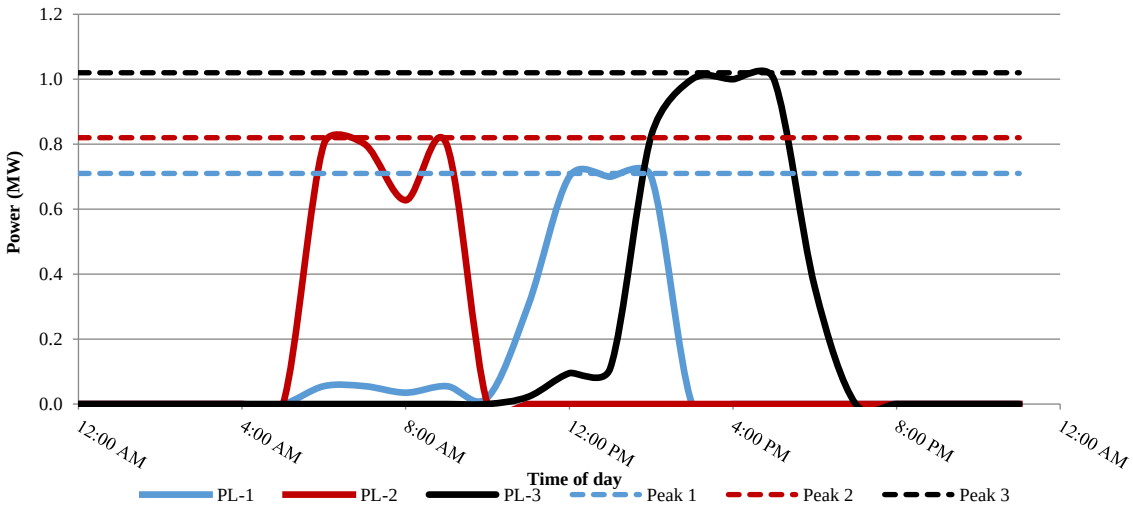


Figure 4.8 MESS results - Power consumed by each PL.

The discharging rate at each PL (in Figure 4.9) varies according to the demand at each time segment and takes a value only if the truck is available at the PL. For PL1, the MESS is available from 11:00 AM to 3:00 PM and discharging with the maximum discharging rate of 200 kW during these four hours and delivering a total of 0.8 MWh, which represents 20% of the total capacity. PL2 receives a total power of 0.71 MW

from 6:00 AM to 10:00 AM, while PL3 share is 0.8 MW from 4:00 PM to 8:00 PM. The algorithm decides to visit PL2 first because its power peak takes place first followed by PL1's and finally followed by PL3's. Figure 4.10 represents the SOC of the battery, noting that the traveling consumption is taken into consideration assuming consumption of 1 kWh/km for the truck, an average speed of 60 km/h, and a 30-km distance between every two consecutive PLs. These assumptions result in 30 minutes of traveling time, the remaining time is assumed for the traffic and setup (connecting/disconnecting) routine. Transit times are expressed by the green color; traveling from PL2 to PL1 takes place from 10:00 AM to 11:00 AM, while traveling from PL1 to PL3 occurs between 3:00 PM to 4:00 PM. Up to 10:00 AM, the MESS is available at PL2 and after 4:00 PM the MESS is available at PL3. PL2 and PL3 receive 17.75% and 20% of the battery capacity, respectively. The final SOC level is 40%. It is worth mentioning that these results depend on market prices, load demand, and traffic in the first place; different values of these study parameters will produce different results.

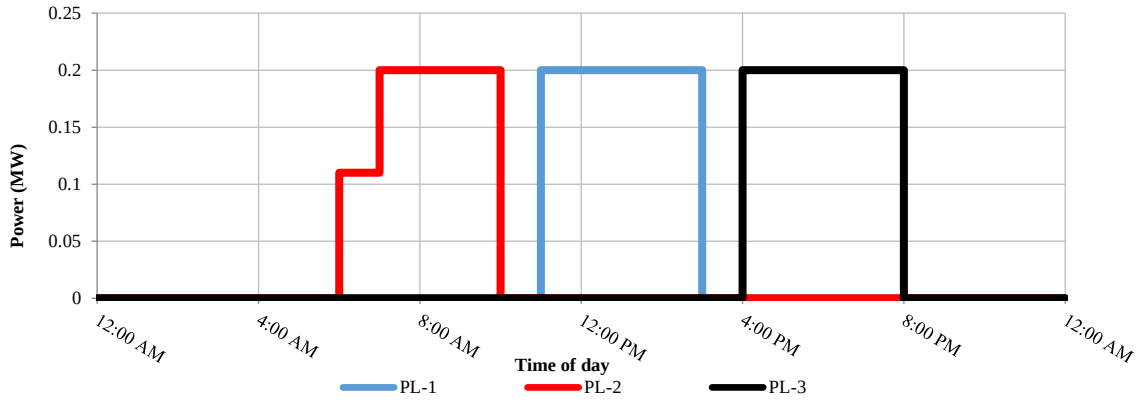


Figure 4.9 MESS discharging rate.

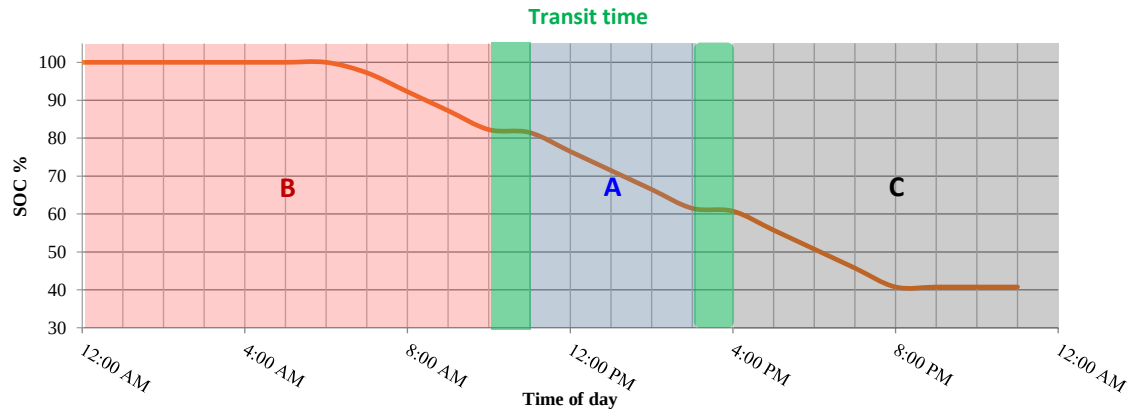


Figure 4.10 MESS results: battery SOC.

**4.2.4 Results discussion.** A summary of the total cost for all case studies is shown in Table 4.3. It turns out that the demand charges are relatively higher than the operating costs, avoiding these charges will result in huge savings. An extra demand cost of $8,781.5 is paid, which represents a 38.6% increase in demand charges in Case 1. In Case 2, using EVs coordination partially shaves the PL peak demands and reduces the demand charges, achieving a total cost of $24,573.49 including an EV charging cost of $495.56 with extra demand charges of $1,327.93. Using the MESS along with the optimal EVs coordination results in a huge reduction in the total operation cost and the savings reach up to 27.7% in comparison with the base case.

Table 4.3 Summary of simulation results.

| | Case 1 | Case 2 | Case 3 |
|---|---|---|---|
| Energy cons. cost | $447.97 | $495.56 | $370.21 |
| Historical peak cost | $22,750 | $22,750 | $22,750 |
| Extra peak charge | $8,781.5 | $1,327.93 | 0 |
| Total cost | $31,979.47 | $24,573.49 | $23,120.21 |
| Savings | - | 23.15% | 27.70% |

## 4.3. Conclusion

Distribution systems are witnessing various challenges due to the rapid increase of EVs. Due to the uncertainty of EVs' charging profiles, many technical issues will take place. This chapter proposes a day ahead scheduling and dispatching of an MESS in conjunction with optimal EVs charging coordination shared by different PLs; each PL should coordinate its charging behavior to have the peak load while the MESS is available at the PL. An MINLP is formulated to minimize the total operation cost and demand charges while satisfying the EVs owners' requests. Different case studies on a real 36 buses radial feeder with real data are used to validate the results and highlight the contribution of the system. The usage of MESS reflected the minimum total operational cost among the discussed case studies while supplying the excess power that exceeds the maximum generation limits if any exists. The usage of the MESS results in savings that reach up to 27.7% in comparison with the base case. The proposed MESS has successfully achieved the objectives, taking into consideration the variants in distribution grids.

# Chapter 5. Optimal Planning of Several MESSs to Serve Multiple EVs Charging Stations

As discussed in the previous chapters, the integration of the MESS and RES technologies is providing a proactive solution to the existing grids to adapt to the increasing penetration of EVs charging power and the dramatically increasing electricity demand. As a result, this deployment creates great challenges as well as opportunities for distribution network planners and operators. In this chapter, an algorithm formulation is proposed for optimum planning of multiple MESS trucks shared among a group of charging stations in order to supply extra demand power and decrease the significant demand charges. The objective of the proposed approach is to replace the tasks of many stationary storage units with a lower number of mobile units that can serve multiple stations during the day. The algorithm optimizes the size and number of trucks required to achieve full supply of the demand and minimum costs for the charging stations' daily operation as well as maintain the maximum profit for the investor. The charging stations are considered to have a PV system that can help in supplying EVs charging demand. A Markov Chain Monte Carlo (MCMC) simulation model is utilized in order to consider uncertainties of PV output power. As the output PV power is time-dependent, i.e., the output of each hour directly depends on the output of the previous hour or state, the MCMC provides an effective modeling scheme to mimic a real-world generation scenario.

## 5.1. Probabilistic Models.

**5.1.1 EV arrivals modeling.** Characteristics of components such as the uncertain nature of RES output power generation should be modeled properly. To that end, a scenario-based approach is deployed in this formulation, where all components are developed based on the assumption that the year is represented by 4 different seasons and each season is represented by a weekday and a weekend. Using the Monte-Carlo simulation, the historical data is used in order to get the parameter of the PDF that best fits the data using the maximum likelihood estimation (MLE) as described in Figure 5.1. Then the inverse CDF method is used to generate N virtual scenarios for each day to be used in the planning process. Figure 5.2 illustrates a sample of the EV arrivals generated scenarios.

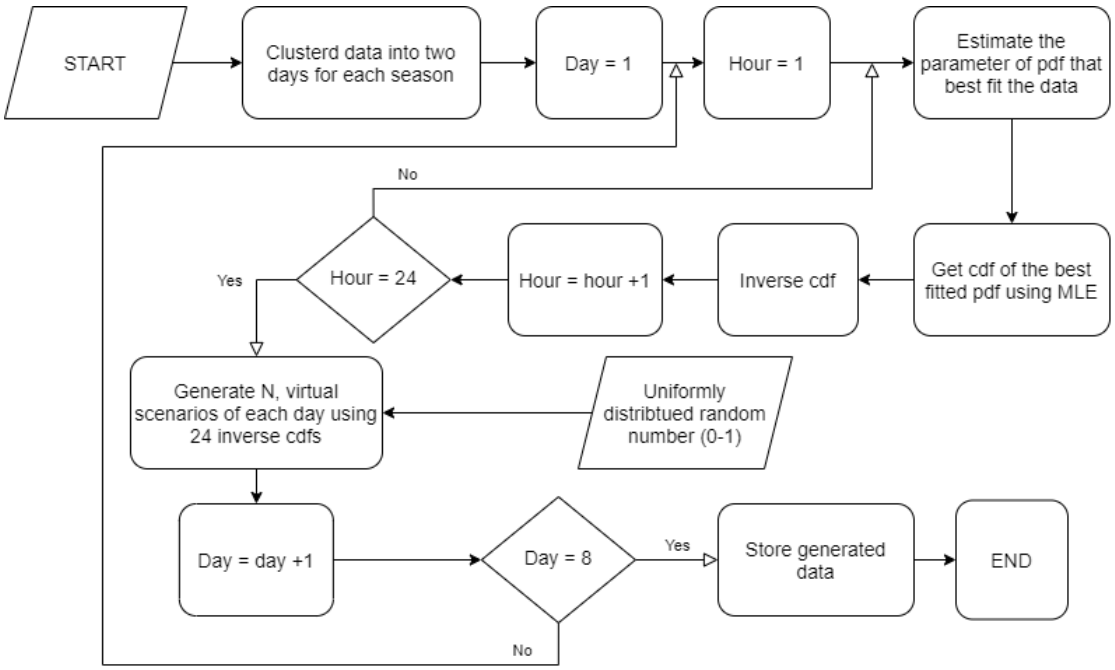


Figure 5.1 Scenario-based EV arrivals model.

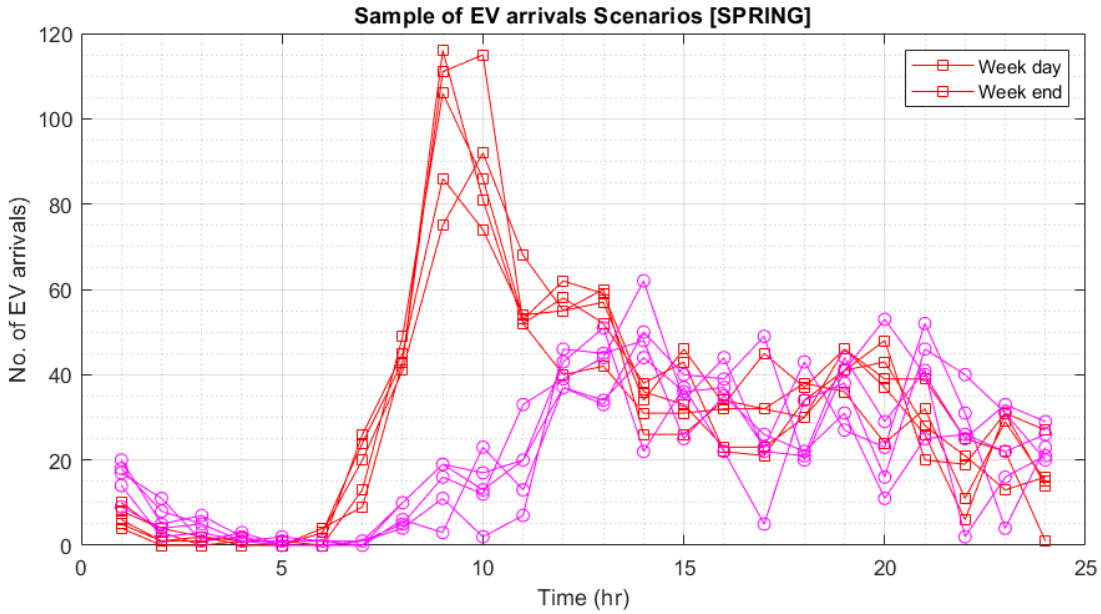


Figure 5.2 EV arrival scenarios sample.

**5.1.2 PV modeling.** PV output power is directly proportional to the solar irradiance and ambient temperature of the site as well as the module characteristics itself. Historical data is used to calculate the output power of these collected data. Output PV power is calculated for each time segment using the following (5.1) – (5.5):

$$T_c = T_A + SIR \times (\frac{NOCT - 20}{0.8}) \quad (5.1)$$

$$I_y = SIR \times [I_{SC} + K_i(T_c - 25)] \quad (5.2)$$

$$V_y = V_{OC} - K_v \times T_c \quad (5.3)$$

$$FF = \frac{V_M \times I_M}{V_{OC} \times I_{SC}} \quad (5.4)$$

$$P_{out} = N_{cell} \times FF \times V_y \times I_y \quad (5.5)$$

where

| | |
|---|---|
| $T_c$ | cell temperature in ℃ |
| $T_A$ | ambient temperature in ℃ |
| $SIR$ | solar irradiance in w/m$^2$ |
| $NOCT$ | nominal operating temperature of cell in ℃ |
| $K_i$ | current temperature coefficient in A/℃ |
| $K_v$ | voltage temperature coefficient in V/℃ |
| $I_{SC}$ | short circuit current in A |
| $V_{OC}$ | open-circuit voltage in V |
| $I_M$ | the current at maximum power point in A |
| $V_M$ | the voltage at maximum power point in V |
| $FF$ | fill factor |
| $P_{out}$ | the output power of the PV module in W |

A defined number of discrete states are defined for SIR where each state represents a range of SIR. The MC simulation will not result in the best output for PV output power since there is no correlation on the temporal space, this is the reason behind using the MCMC simulation in PV modeling. In this method, a transition matrix T is built for each time segment in each day within each season. This will result in a total of $4 \times 12 = 48$ matrices. Each element $T_{xy}$ in T represents the probability of state

$y$ to take place at time segment t under the condition that the state at $t-1$ is known to be $x$ [53]. These conditional probabilities are calculated as in (5.6):

$$T_{xy} = P\left(\frac{Z_t = y}{Z_{t-1} = x}\right) = \frac{n_{xy}}{\sum_k n_{xy}}, \forall\, x, y \tag{5.6}$$

where $n_{xy}$ is the number of transitions from state $x$ at time $t-1$ to state $y$ at time segment $t$. After calculating all the transition matrices, the cumulative transition matrices $\mathbf{T_c}$ are obtained, the elements of which are defined as in (5.7).

$$T_{c,xy} = \sum_{r=1}^{y} T_{xy}\ , \forall\, x, y \tag{5.7}$$

Both types of matrices representing all possible states of SIR in the system which can be used to generate as many annual scenarios as needed using the inverse cumulative distribution function (CDF) method. The output states are mapped to the actual PV output power as a final step. As a result of the algorithm, any number of scenarios can be obtained using the limited historical data while ensuring that the scenarios are following the same distribution. The presented model is used to ensure a chronologically based change between the state as each state is directly dependent on the previous state. In this model of PV output power, many hours of the day can be neglected since there is no output power during the night, this might help in reducing the computational time and ensuring that the resulting scenarios are reliable. Transition matrices and cumulative transition matrices will have a probability of 1 for this state of zero output power since there is no other probability to generate any amount of power in the absence of sunlight. As PV output power directly depends on the SIR, it is also affected by the season of the year. Since some seasons receive a higher SIR range than the others, for example, spring. Figures 5.3 - 5.6 show a comparison between samples of real and generated scenarios data of PV generations output power during different seasons of the year. The MCMC model successfully mimicked the real data and can provide a pretty good estimation of PV power generation to be used in the planning problem.

According to the comparison between the real and generated samples, the state probabilistic model is robust and can be used in case studies to mimic a real-world PV generation.

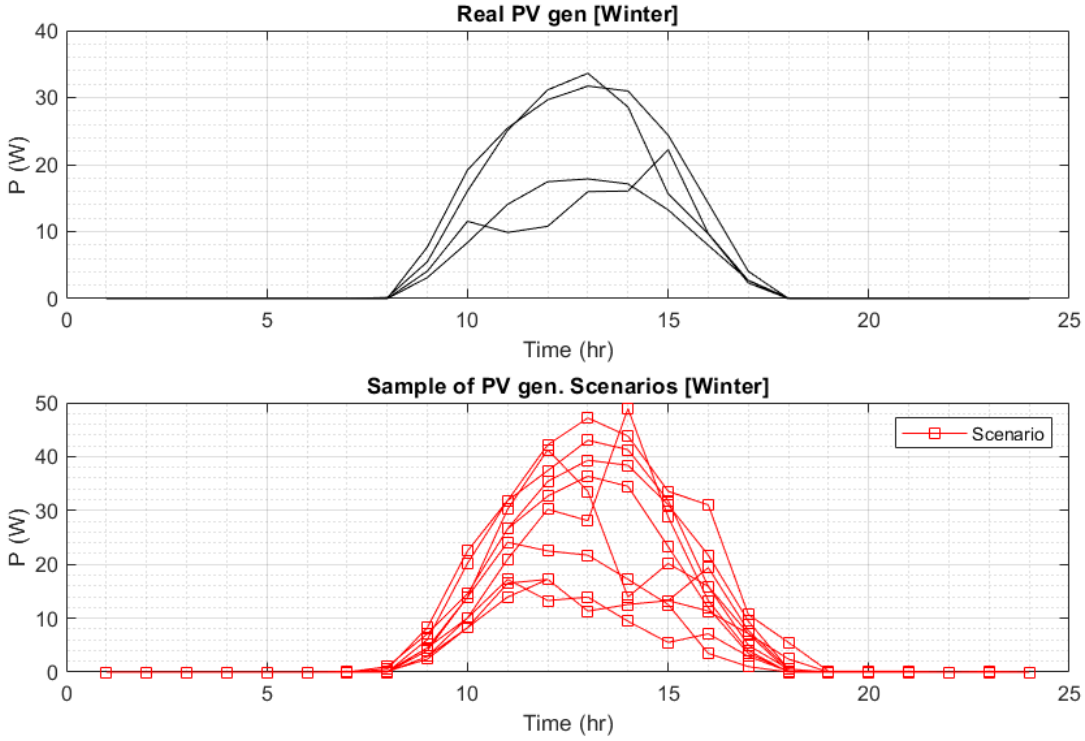


Figure 5.3 Comparison between real and generated scenario PV output power in winter.

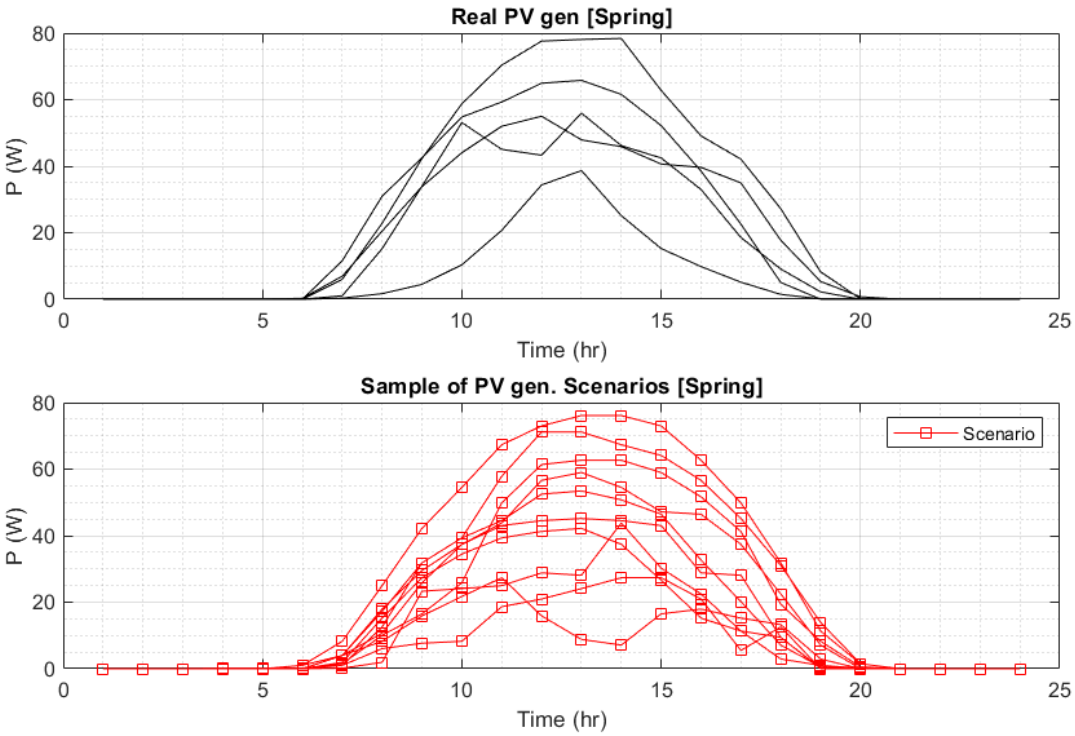


Figure 5.4 Comparison between real and generated scenario PV output power in spring.

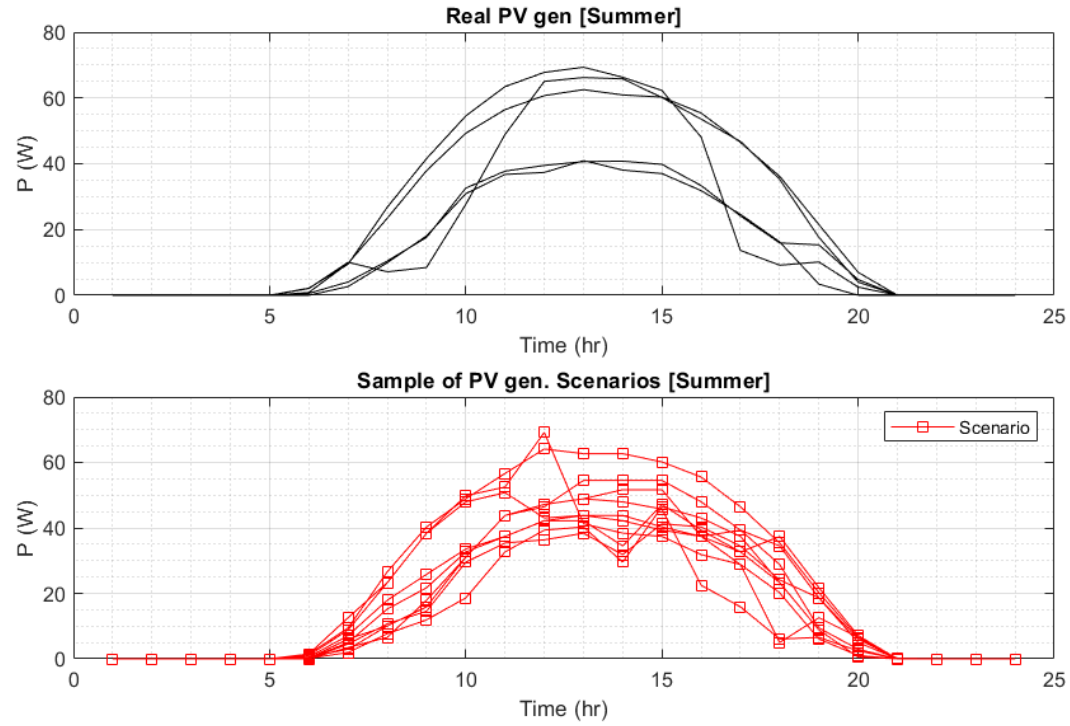


Figure 5.5 Comparison between real and generated scenario PV output power in summer.

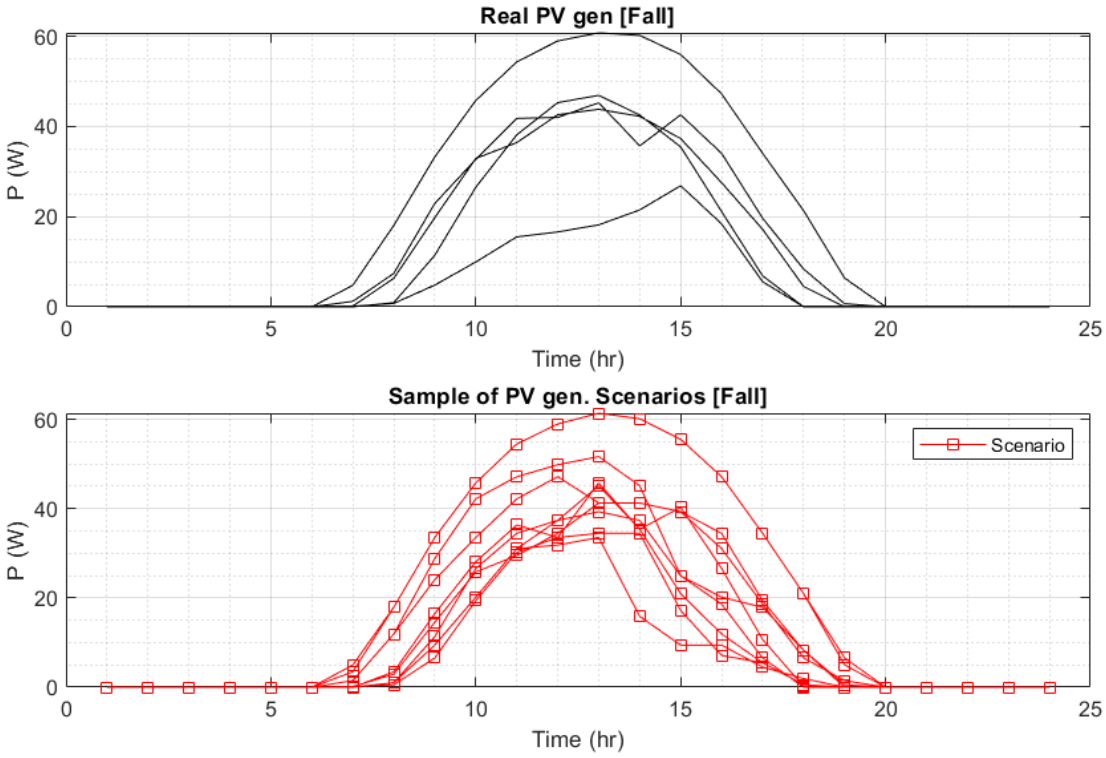


Figure 5.6 Comparison between real and generated scenario PV output power in fall.

## 5.2. Problem Formulation

To simplify the formulation, the following terminology is used. For any variable $x_t^y$, $x$ is the variable name (e.g., $p$: power); $y$ represents the associated label/description (e.g., $DCH$: discharge); finally, $t$ is the indices associated to that variable (e.g., $s$: charging station index). The objective function of this planning formulation is to find the optimum number of MESSs to be involved in the project as well as the optimum capacity of each MESSs' battery packs while meeting all charging station power demand and minimize the operational costs and demand charges.

The minimization of the total capital and operational costs of the project, since the income can be the fees paid by each charging station to be served by the MESS fleet, is the main objective. Then the profit can be calculated easily as the difference between costs and incomes. In this study, the participating charging stations are considered to finance the project. The objective function of the model illustrated in (5.8) represents the minimization of the annualized capital and operation cost of the project. To ensure that each of these costs is accurately represented, the capital costs are represented by equal annualized payments over the lifetime of the project, $lt$, using the capital recovery factor (CRF) as in (5.9), while the levelization factor (LF) in (5.10) is used to represent all annualized operational costs to be paid in the future [54], as follows:

$$\min C^{cost} + O\&M^{cost} \tag{5.8}$$

$$CRF = \frac{d(d+1)^{lt}}{(d+1)^{lt}-1} \tag{5.9}$$

$$LF = CRF \times \frac{(d'+1)^{lt}-1}{d'(d+1)^{lt}}, \qquad d' = \frac{d-e}{e+1} \tag{5.10}$$

where $d$ is the discount rate, $d'$ is the effective discount rate, and $e$ is the escalation rate.

The annualized capital cost $C^{cost}$ can be found using (5.11) which consists of

1- The truck capital cost $CC^{MS}$ multiplied by the maximum number of trucks used in the daily operation algorithm.

2- The battery capacity cost of each truck multiplied by the battery bank cost $B^{cost/MWh}$. The parameter $\alpha^N$ is set to compensate for the future battery extension or replacement cost; defined as reaching a certain number of cycles

$N$ by the end of the project lifetime $lt$ [55].

$$C^{cost} = CRF \times [\sum_{k} A_k \times CC^{MS} + \sum_{k} E_k^{MS} \times B^{cost/MWh} \times (1+\alpha^N)\,] \quad (5.11)$$

$$O\&M^{cost} = LF \times [M^{cost} + \sum_{se=1}^{4} N_{se}^{days} \left(\frac{5}{7} \times C_{se}^{daily,wd} + \frac{2}{7} \times C_{se}^{daily,we}\right)] \quad (5.12)$$

The operation and maintenance costs $O\&M^{cost}$ as shown in (5.12) consist of

1- The daily operational cost of the weekdays $C^{daily,wd}$ and weekends $C^{daily,we}$, where $N_{se}^{days}$ is the number of days in each season $se$.
2- The fixed operational and maintenance cost $M^{cost}$ consists of the drivers' salaries and trucks' maintenance cost.

**5.2.1 Operational algorithm of multiple MESSs.** The objective function of the operational algorithm shown in (5.13) aims at minimizing the total cost of the total drained power by the PLs to charge the arrival EVs and the total demand charges for each charging station $\boldsymbol{s}$. As shown in (5.14), the historical peak demand $\boldsymbol{P_s^{MAX-Target}}$ is used to calculate the demand charges, the extra peak demand charges are only considered for the power exceeds the $\boldsymbol{P_s^{MAX-Target}}$. The additional demand charges $\boldsymbol{C^{peak}}$ will be considered to be zero if the peak is not exceeding the historical peak demand, as follows:

$$\min \sum_{s} \left( \sum_{t \in \mathbb{T}} \left( C_t^{grid} P_{s,t}^{ev} \Delta t \right) + C_s^{peak} \right) \quad (5.13)$$

$$C_s^{peak} = \begin{cases} 0 & , \forall \left( P_s^{ev-MAX} - P_s^{MAX-Target} \right) \leq 0 \\ C^{kw} \left( P_s^{ev-MAX} - P_s^{MAX-Target} \right) & , otherwise \end{cases} , \forall\, s \quad (5.14)$$

where $C_t^{grid}$ refers to the variable grid cost at each time interval; $P_{s,t}^{ev}$ is the total power consumed by EVs at each bus and each time interval; $\mathbb{T}$ is the set of all the time segments; $C_s^{peak}$ is the total extra peak demand charges for charging stations $s$; $C^{kw}$ is the demand charges in \$/kW; $P_s^{ev-MAX}$ is the peak demand of the charging stations $s$; $P_s^{MAX-Target}$ is the historical recorded or targeted recorded peak demand.

***5.2.1.1 EV charging constraints.*** Equation (5.15) describes the total power for each charging station. The first term in (5.16) represents the required EVs

charging power; the second term is the power injected from the MESS to each PL. Charging decisions are restricted by the availability of the EV and it can take a value from zero up to the full charging rate as in (5.16), as follows:

$$P_{s,t}^{L-EV} = \left( \sum_{v \in \mathbb{V}_s} \frac{X_{v,s,t}^{EV} \, P_v^{CH}}{\eta_{ch} \, S^{base}} \right) - P_{k,s,t}^{DCH-MS} - PV_{s,t}, \forall \, s, t \tag{5.15}$$

$$\begin{aligned} X_{v,s,t}^{EV} &\leq A_{v,s,t} \, , \forall \, v, s, t \\ 0 \leq X_{v,s,t}^{EV} &\leq 1, \forall \, v, s, t \end{aligned} \tag{5.16}$$

where $v$ and $\mathbb{V}_s$ are the index and the subset of chargers of charging station $s$, respectively; $X_{v,s,t}^{EV}$ is the charging decision as a fraction of the charger capacity; $P_v^{CH}$ is the charger capacity in kW; $\eta_{ch}$ is the efficiency of charging; $S^{base}$ is the system base power in kVA for the per-unit system; $A_{v,s,t}$ is a binary parameter indicating whether charger $v$ of charging station $s$ is occupied with an EV at time $t$, i.e. if $A_{v,s,t} = 1$, then an EV is plugged into the charger; $P_{s,t}^{MS}$is the power injected from the MESS.

The state of charge (SOC) of each EV is updated with the charging energy as in (5.17) and (5.18). Equation (5.19) is used to ensure satisfying the pre-required demand for each EV.

$$SOC_{v,s,t}^{EV} = SOC_{v,s,t-1}^{EV} + \Delta SOC_{v,s,t}^{EV} \tag{5.17}$$

$$\Delta SOC_{v,s,t}^{EV} = \frac{X_{v,s,t}^{EV} \, P_v^{CH-EV} \Delta T}{E_{v,s}^{BAT}} \tag{5.18}$$

$$SOC_{v,s,t}^{EV} \leq SOC_{v,s}^{REQ} \tag{5.19}$$

where $SOC_{v,s,t}^{EV}$is the SOC at time $t$ for each EV; $\Delta SOC_{v,s,t}^{EV}$ the change in the SOC due to charging; $\Delta T$ is the time segments in hours; $E_{v,s}^{BAT}$is the battery capacity in kWh; $SOC_{v,s}^{REQ}$is the required SOC by each EV driver.

***5.2.1.2 Multiple MESSs formulation.*** The algorithm used in this formulation is different than the previously introduced model as this approach optimizes the number of MESSs to be dispatched to serve several charging stations involved in a pre-assigned agreement. There are three different binary variables are involved to represent this model. $A_k$ represents the index of MESS out of k MESSs available to be dispatched during the day, this is equivalent to the minimum number of

trucks required to meet the daily demand of the assigned charging stations. $B_{k,s}$ represents the assignment of each charging station s to be served by MESS k. Finally, $C_{k,s,t}$ to decide the availability of the MESS $k$ at charging station s at time segment t.

The constraint in (5.20) states that each charging station $s$ will be assigned to be served by only one MESS. Constraints (5.21) - (5.23) ensure that all involved charging stations will be served by an MESS.

$$\sum_{k \in \mathrm{K}} B_{k,s} = 1, \forall\, s \tag{5.20}$$

$$\sum_{s \in \aleph} B_{k,s} \leq \aleph \times A_k, \forall\, k \tag{5.21}$$

$$\sum_{t \in \mathbb{T}} C_{k,s,t} \leq \aleph \times B_{k,s}, \forall\, k, s \tag{5.22}$$

$$\sum_{k,t} C_{k,s,t} \geq 1, \forall\, s \tag{5.23}$$

where K is the maximum number of MESSs and $\aleph$ is the total number of charging stations to be served.

When the MESS is in transit or at any parking lot, the SOC of the MESS battery is updated as in (5.24) and (5.25) at each time segment. It is affected by the injected energy and the MESS traveling consumption, as follows:

$$SOC_{k,t}^{MS} = SOC_{k,t-1}^{MS} + \Delta SOC_{k,t}^{MS} \tag{5.24}$$

$$\Delta SOC_{k,t}^{MS} = \frac{(\sum_s P_{k,s,t}^{C-MS} - \sum_s P_{k,s,t}^{DCH-MS} - \sum_{s,s'} P_{k,s,s',t}^{T-MS})\Delta T}{E_k^{MS}} \tag{5.25}$$

Equation (5.26) maintains the battery limits, as follows:

$$SOC_{k,t}^{MS-MIN} \leq SOC_{k,t}^{MS} \leq 1.0 \tag{5.26}$$

where $SOC_{k,t}^{MS}$ is the SOC of the MESS $k$ battery at time $t$; $\Delta SOC_{k,t}^{MS}$ is the change in the SOC due to charging, discharging, and traveling; $P_{k,s,t}^{C-MS}$ and $P_{k,s,t}^{DCH-MS}$ are the charging and discharging rates of truck $k$ in charging station $s$ at time segment $t$, respectively; $P_{k,s,s',t}^{T-MS}$ is the power consumed due to traveling between charging station $s$ and charging station $s'$ for truck $k$ at time $t$; $E_k^{MS}$ is the battery capacity in kWh for each truck $k$; $SOC_{k,t}^{MS-MIN}$ is the minimum SOC of the truck $k$.

The power delivered $P_{k,s,t}^{DCH-MS}$ by truck $k$ to charging station $s$ at time $t$ depends on the availability variable $C_{k,s,t}$ as illustrated in (5.27). The traveling time between the charging stations is merged in this model during the first discharging time segment, i.e., discharging power in charging station $s$ at $t = 1$ will be less than the maximum possible discharging power $P_k^{DCH-max}$ by a factor $F_{s,s\prime}$ to compensate for the traveling time. $F_{s,s\prime}$ is a square matrix that has a diagonal of zeros, while the remaining elements are fractions between [0-1] depends on the distances between the charging stations. $T_{k,s,s',t}^{MS}$ represents the fraction of the maximum possible discharging power to be discharged at charging station $s$ at $t = 1$ as explained in (5.28). The explanation of how the binary variable $x_{k,s,s',t}$ captures the traveling time segment between charging stations $s$ and $s'$ is presented in (5.30) - (5.32). Equation (5.29) calculates the power drained from the tuck $k$ while traveling between charging stations $s$ and $s'$ for each time segment. This drained power is directly related to the distances between the charging stations, the traffic, and the speed of the truck. These factors can be considered together while developing the distance matrix $D_{s,s\prime}$.

$$P_{k,s,t}^{DCH-MS} \leq P_k^{DCH-max} \times C_{k,s,t} - \sum_{s\prime} T_{k,s,s',t}^{MS} \ , \forall\, k, s, t \tag{5.27}$$

$$T_{k,s,s',t}^{MS} = F_{s,s\prime} \times P_k^{DCH-max} \times x_{k,s,s',t} \ \forall\, k, s, s', t \tag{5.28}$$

$$P_{k,s,s',t}^{T-MS} = D_{s,s\prime} \times x_{k,s,s',t} \ \forall\, k, s, s', t \tag{5.29}$$

To capture the traveling time segment, the set of linear equations (5.30) - (5.32) are developed, as follows:

$$x_{k,s,s',t} \geq C_{k,s,t} + C_{k,s',t} - 1 \ , where\ t \geq 2 \tag{5.30}$$

$$x_{k,s,s',t} \leq C_{k,s,t} \ , where\ t \geq 2 \tag{5.31}$$

$$x_{k,s,s',t} \leq C_{k,s',t+1} \ , where\ t \geq 2 \tag{5.32}$$

These linear equations are replacing a single simpler but non-linear equation to keep the model linear. The previous set of constraints can be used to capture the change in the variable $C_{k,s,t}$ (i.e., travel between charging stations) by each truck $k$ at time $t$. The previous explained linear operation model results in the total daily cost of the charging station served by multiple MESSs while meeting the EV's charging demands and minimizing the demand charges for each charging station.

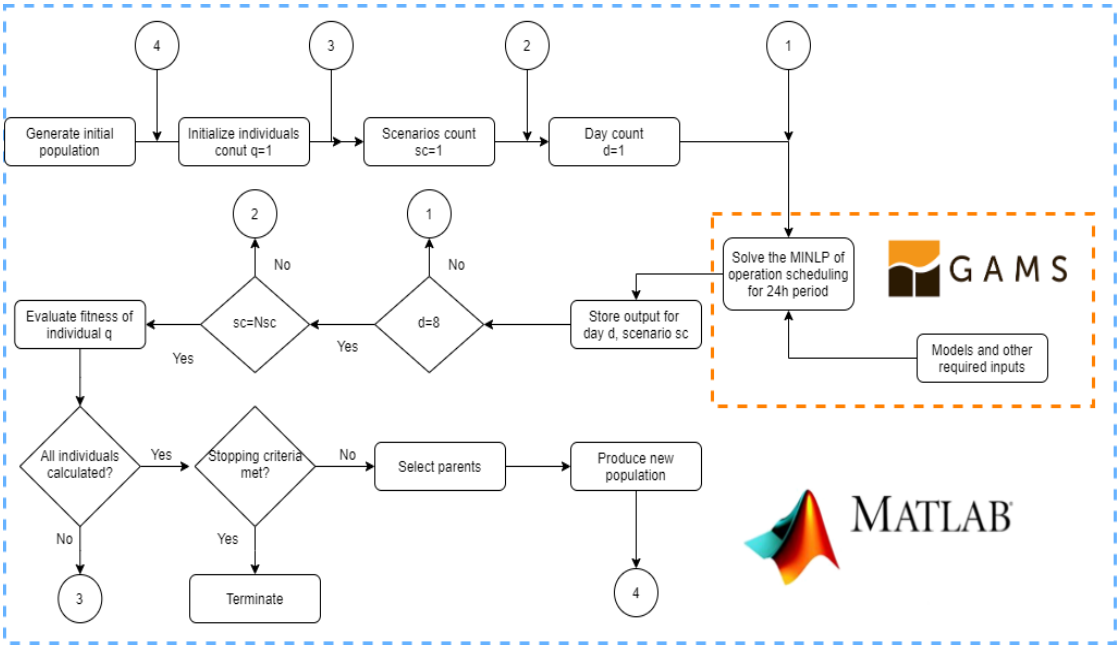


Figure 5.7 Solution approach.

The problem formulated is divided into two problems, outer problem and inner problem. The inner problem is solving the daily operational algorithm using a deterministic approach under the GAMS environment, while the outer problem is solving for optimal sizes using a metaheuristic approach under the MATLAB environment. The operational model is fed with daily data for each season as illustrated in Figure 5.7, then the outputs as gathered for each scenario and evaluate the fitness function for all individuals. The last step is checking for the stopping criteria to terminate. The stopping criteria used is the change in the fitness function, if the change is less than a certain threshold, then the program stops.

## 5.3. Case Study

The MESSs' algorithm is validated by simulating a case study involving five different charging stations assumed to participate in the project. The optimization inputs consist of the rated power of PV panels installed at each charging station and the MESSs' input data are given in Table 5.1. The PV solar irradiance historical data utilized in the model is available in [56], while a real market energy price is taken from [57] and shown in Figure 5.8. In order to account for the transition phase of the MESSs', the truck average speed is assumed 60 km/h, the traveling time between the charging stations in this case study is assumed to be equal for simplicity, which means equal distances between charging stations are considered. It is assumed that each charging

station has a PV plant that supports supplying the required demand. Six years of solar irradiance and temperature data are used in the algorithm to cover the whole planning horizon. In order to avoid increasing problem complexity, the k-means clustering method approximates the data to a defined number of states to be used in scenarios' generation.

For the MESSs, the lithium-ion battery is used due to its small size (i.e., high energy intensity) and long battery life. The storage life cycles are assumed to be 3000 cycles during the planning period which is assumed to be 12 years. The yearly operation and maintenance cost is assumed to be 40k$/year including the drivers' salaries and insurance, this cost is per truck.

Table 5.1 Optimization input parameters.

| **Optimization input parameters** | |
|---|---|
| $B^{cost/MWh}$ | 600k$ |
| $CC^{MS}$ | 50k$ |
| $d$ | 4% |
| $e$ | 2% |
| $M^{cost}$ | 40k$/year |
| $lt$ | 12 years |
| $\alpha^{N}$ | 15% |

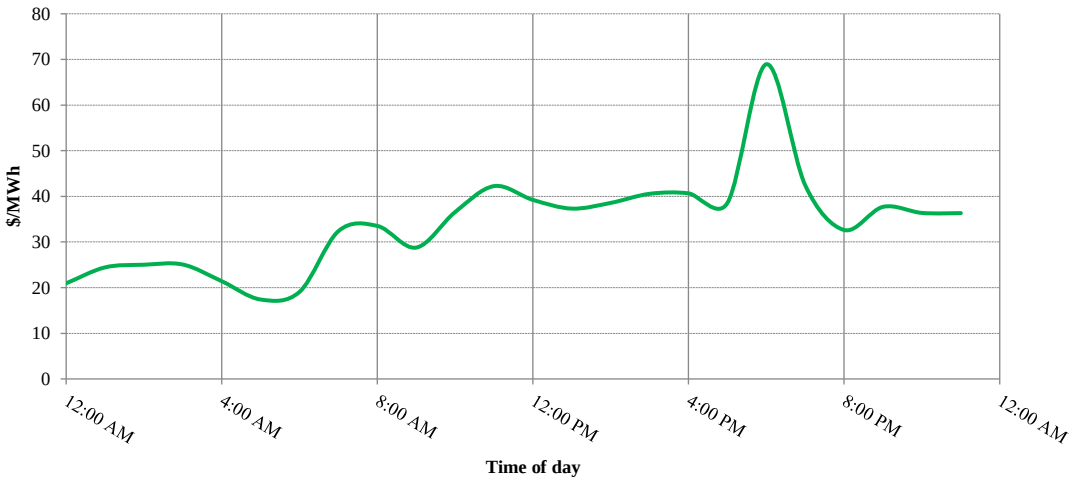


Figure 5.8 Energy price.

Figure 5.9. shows the comparison of the total drained power of the grid for the

participating charging station with and without the integration of the MESSs, the fleet of MESSs manage to reduce the total power demand of the served charging station which will not only reduce the demand charges, but also will supply and extra required energy that exceeds the generation limits. It is shown that the huge saving takes place in the highest price hours (peak hours). The peak demand reduced from 2 MW in the absence of the MESSs to 1.62 MW. The model decides to use two MESSs as an optimal solution, MESS-1 to serve the third and fourth charging stations, while MESS-3 serves the first, second, and fifth charging stations as shown in Figure 5.8.

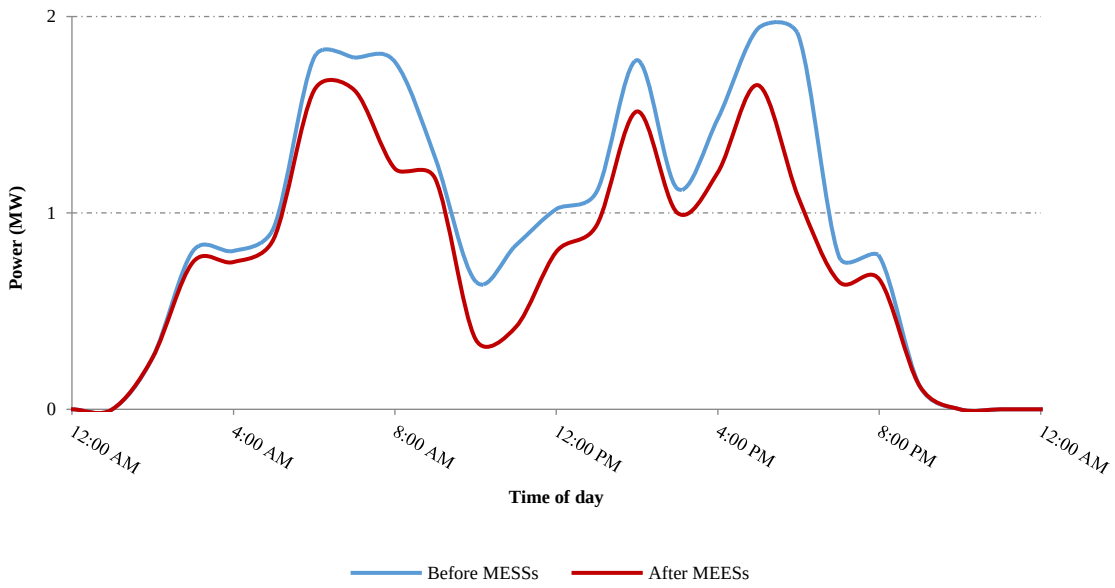


Figure 5.9 Total charging stations power drained from the grid.

To judge the dynamic performance of the model, a random day scenario, presented in Figures 5.10, 5.11, and 5.12, illustrates the SOC of the dispatched MESSs. MESS-3 discharged the full capacity and reached the minimum SOC which is 20%, while MESS-1 reached 52% of the total capacity. The green part on the figures shows the traveling phase of the MESS between parking lots; however, the energy consumption during the traveling is considered in the discharging rate of the first hour at each charging station as explained earlier in section 5.1. Table 5.2 shows the economic results and the savings results out of integrating the model.

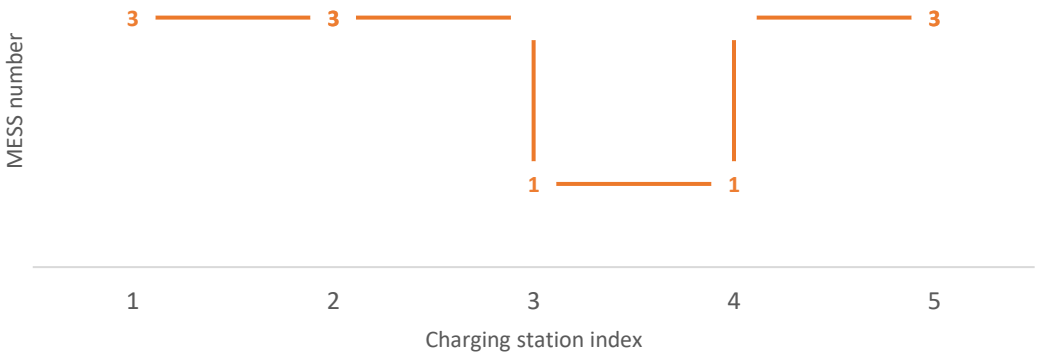


Figure 5.10 Charging stations assigned to MESSs.

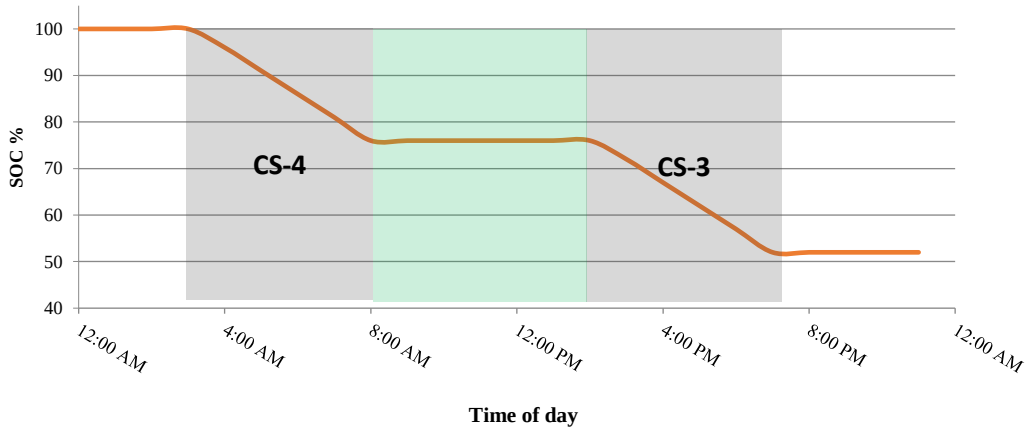


Figure 5.11 MESS 1 - SOC.

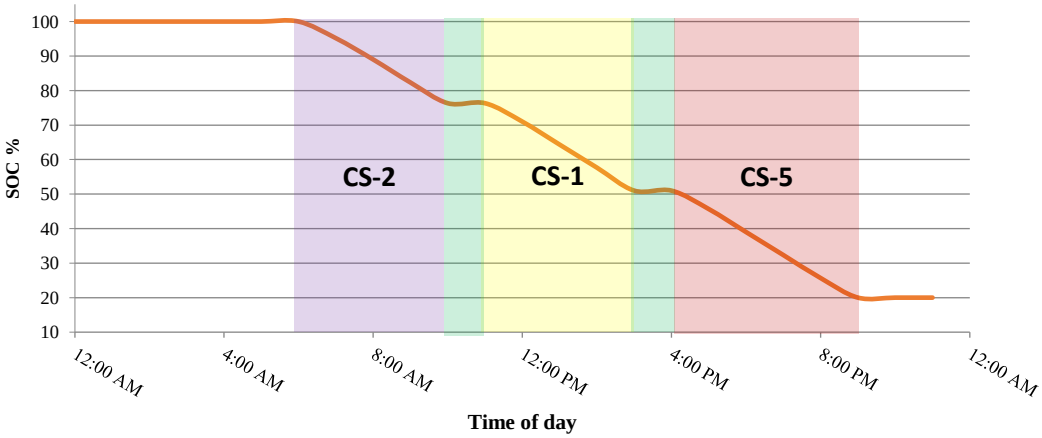


Figure 5.12 MESS 3 - SOC.

The model decides to dispatch two MESSs out of the available, with 3.031-MWh and 3.125-MWh capacity, respectively. Considering the capital costs mentioned in Table 5.1, the resulting battery bank cost and MESSs capital cost involved in the

project are $3,693,840 and $3,793,840, respectively. The demand charge rate is considered to be 9.1$/kWh, considering that, the annual operation cost without model integration is found to be $1,051,737.12. On the other hand, the annual operation cost taking into consideration the annualized capital cost and levelized daily operation cost is $963,480.07. As a result, $88,257.05 is saved which represents 8.39% total savings out of model integration. Besides the financial savings, the usage of these MESSs will allow the charging stations involved to accommodate higher penetration of EVs and supply the increasing charging demand, which will avoid or, at least, delay the upgrade of the system infrastructure. This can be concluded easily from the peak demand reduction of 19% as shown in Table 5.2.

Table 5.2 Optimization results.

| **Optimization results** | | |
|---|---|---|
| $A_k$. | | {1, 0, 1, 0} |
| $E_1^{MS}$. | | 3031.4 kWh |
| $E_3^{MS}$. | | 3125 kWh |
| Battery bank cost | | $3,693,840 |
| MESSs capital cost | | $3,793,840 |
| Peak reduction | | 19% |
| Demand charge | | 9.1$/kWh |
| Annual operating cost | without MESSs | $1,051,737.12 |
| | with MESSs | $963,480.07 |
| Annual savings | | $88,257.05 |
| Savings percentage | | 8.39% |

# Chapter 6. Conclusions

## 6.1. Concluding Remarks

This thesis proposes and discusses different approaches utilizing mobile energy storage technology in the power system. The primary objective in all the proposed approaches aims at minimizing the total operation cost while satisfying all EVs charging station demand. In addition to providing a solution to the necessary infrastructure upgrades to accommodate the increasing penetration of EVs.

A solution to the existing charging stations is proposed in Chapter 3 which utilizes an MESS to serve charging stations. A couple of case studies were discussed in order to highlight the contribution of the proposed algorithm. The proposed algorithm has successfully reduced the total operational cost of the PLs associated with the case study. In Chapter 4, a dynamic optimization algorithm that controls the charging behavior of EVs and takes the MESS availability at each location into consideration is presented. It can be defined as a day ahead scheduling and dispatching of an MESS in conjunction with optimal EVs charging coordination shared by different PLs; each PL should coordinate its charging behavior to have the peak load while the MESS is available at the PL. An MINLP is formulated to minimize the total operation cost and demand charges while satisfying the EVs owners' requests. Different case studies on a real 36 buses radial feeder with real data are used to validate the results and highlight the contribution of the system. In Chapter 5, a planning algorithm is proposed that utilizes the integration of an optimum number and their battery bank capacities to serve to participate charging stations to accommodate for the increasing charging demand and minimize the total operation cost, taking into consideration all the assets, costs, and variabilities of the involved component.

## 6.2. Future Work

The following recommended research directions can be a suitable extension out of this thesis:

1. Large scale implementation by expanding the serving fleet.
2. The inclusion of a detailed transit delay model in the planning process of MESSs.
3. The usage of the MESSs in voltage regulation and grid support at critical buses.

## References


[1] “Electric Vehicle Market,” Market Research Firm. Available: https://www.marketsandmarkets.com/Market-Reports/electric-vehicle-market-209371461.html. Jun-2019 [Oct. 4, 2020].

[2] S. Babaei, D. Steen, T. A. Le, O. Carlson, and L. Bertling, “Effects of plug-in electric vehicles on distribution systems: A real case of Gothenburg,” in *Proc. IEEE Innov. Smart Grid Technol. Conf.Eur*, Gothenburg, Sweden, Oct. 2010, pp. 1–8.

[3] I. T. Papaioannou, A. Purvins, and E. Tzimas, “Demand shifting analysis at high penetration of distributed generation in low voltage grids,” *Elect. Power Energy Syst.*, vol. 44, no. 1, pp. 540–546, June, 2013.

[4] J. Eyer and G. Corey, "Energy Storage for the Electricity Grid: Benefits and Market Potential Assessment Guide," *SANDIA National Laboratories*, United States of America, 2010.

[5] "Office of Energy and Efficiency and Renewable Energy," EERE www.energy.gov, 8 December 2020 [Jan. 4, 2021].

[6] P. Sanchez-Martin, G. Sanchez and G. Morales-Espana, "Direct Load Control Decision Model for Aggregated EV Charging Points," *IEEE Trans Power Syst.*, vol. 27, no. 3, pp. 1577-1584, Feb. 2012.

[7] W. Tushar, C. Yuen, S. Huang, D. B. Smith, and H. V. Poor, "Cost Minimization of Charging Stations With Photovoltaics: An Approach With EV Classification," *IEEE Trans. Intell Trans Syst*, vol. 17, no. 1, pp. 156-169, June 2016.

.

[8] A. Khaligh and Z. Li, "Battery, Ultracapacitor, Fuel Cell, and Hybrid Energy Storage Systems for Electric, Hybrid Electric, Fuel Cell, and Plug-In Hybrid Electric Vehicles: State of the Art," *IEEE Transactions on Vehicular Technology*, vol. 59, no. 6, pp. 2806-2814, Aug 2010.

[9] C. C. Chan, A. Bouscayrol, and K. Chen, "Electric, Hybrid, and Fuel-Cell Vehicles: Architectures and Modeling," *IEEE Transactions on Vehicular Technology*, vol. 59, no. 2, pp. 589-598, Sep 2010.

[10] H. Saboori, R. Hemmati, S. M. S. Ghiasi, and S. Dehghan, "Energy storage planning in electric power distribution networks – A state-of-the-art review," *Renewable and Sustainable Energy Reviews*, vol. 79, pp. 1108-1121, Nov. 2017.

[11] C. Christiansen and B. Murray, "Energy Storage Study," http://arena.gov.au/assets/2015/07/AECOM-Energy-Storage-Study.pdf, Aug, 2015 [December 8, 2020].

[12] D. Infield and J. Hill. (2015, October 1), *Literature Review: Electrical Energy Storage for Scotland, Institute of Energy and Environment*. (1st edition). [Online]. p 53. Available: https://pureportal.strath.ac.uk/en/publications/literature-review-electrical-energy-storage-for-scotland [April 1, 2021].

[13] S. Vazquez, S. M. Lukic, E. Galvan, L. G. Franquelo, and J. M. Carrasco, "Energy Storage Systems for Transport and Grid Applications," *IEEE Transactions on Industrial Electronics*, vol. 57, no. 12, pp. 3881-3895, July 2010.

[14] H. H. Abdeltawab and Y. A. R. I. Mohamed, "Mobile Energy Storage Scheduling and Operation in Active Distribution Systems," *IEEE Transactions on Industrial Electronics*, vol. 64, no. 9, pp. 6828-6840, Aug 2017.

[15] Y. S. Wong, L. L. Lai, S. Gao, and K. T. Chau, "Stationary and mobile battery energy storage systems for smart grids," in *2011 4th International Conference on Electric Utility Deregulation and Restructuring and Power Technologies*, July 2011, pp. 1-6..

[16] C. W. Gellings, "The concept of demand-side management for electric utilities," in *Proceedings of the IEEE*, vol. 73, no. 10, pp. 1468-1470, Oct. 1985.

[17] M. Pipattanasomporn, S. Rahman, and S. Shao, "Grid integration of electric vehicles and demand response with customer choice," *IEEE Trans. Smart Grid*, vol. 3, no. 1, pp. 543–550, Mar. 2012.

[18] E. Sortomme and M. A. El-Sharkawi, "Optimal charging strategies for unidirectional vehicle-to-grid," *IEEE Trans. Smart Grid*, vol. 2, no. 1, pp. 131–138, Mar. 2011.

[19] K. Clement, E. Haesen, and J. Driesen, "The impact of vehicle-to-grid on the distribution grid," *Elect. Power Syst. Res*., vol. 81, no. 1,pp. 185–192, Jun. 2011.

[20] W. Kempton and J. Tomi, "Vehicle-to-grid power implementation: From stabilizing the grid to supporting large-scale renewable energy," *J. Power Sources*, vol. 144, no. 1, pp. 280–294, Jun. 2005.

[21] L. Hua, J. Wang and C. Zhou, "Adaptive Electric Vehicle Charging Coordination on Distribution Network," in *IEEE Transactions on Smart Grid*, vol. 5, no. 6, pp. 2666-2675, Nov. 2014.

[22] H. Kikusato et al., "Electric Vehicle Charging Management Using Auction Mechanism for Reducing PV Curtailment in Distribution Systems," in *IEEE Transactions on Sustainable Energy*, vol. 11, no. 3, pp. 1394-1403, July 2020.

[23] S. Tong, T. Fung, and J. W. Park, “Reusing electric vehicle battery for demand side management integrating dynamic pricing,” in *2015 IEEE International Conference on Smart Grid Communications*. March 2015, pp. 325–330.

[24] M. Moeini-Aghtaie, A. Abbaspour, M. Fotuhi-Firuzabad, and P. Dehghanian, “Optimized Probabilistic PHEVs Demand Management in the Context of Energy Hubs,” *IEEE Trans. Power Deliv.*, vol. 30, no. 2, pp. 996–1006, Apr. 2015.

[25] N. G. Paterakis, A. Tascikaraoglu, O. Erdinc, A. G. Bakirtzis, and J. P. S. Catalao, “Assessment of Demand-Response-Driven Load Pattern Elasticity Using a Combined Approach for Smart Households,” *IEEE Trans. Ind. Inform.*, vol. 12, no. 4, pp. 1529–1539, Aug. 2016.

[26] S. Faddel and O. A. Mohammed, "Automated Distributed Electric Vehicle Controller for Residential Demand Side Management," in *IEEE Transactions on Industry Applications*, vol. 55, no. 1, pp. 16-25, Jan.-Feb. 2019.

[27] J. Zhang et al., "A Hierarchical Distributed Energy Management for Multiple PV-Based EV Charging Stations," *IECON 2018 - 44th Annual Conference of the IEEE Industrial Electronics Society*, Washington, DC, 2018, pp. 1603-1608.

[28] R. R. Deshmukh and M. S. Ballal, "An energy management scheme for grid connected EVs charging stations," *2018 International Conference on Power, Instrumentation, Control and Computing*, 2018, pp. 1-6.

[29] A. Alsabbagh and C. Ma, "Distributed Charging Management of Electric Vehicles Considering Different Customer Behaviors," in *IEEE Transactions on Industrial Informatics*, vol. 16, no. 8, pp. 5119-5127, Aug. 2020.

[30] Q. Yan, B. Zhang and M. Kezunovic, "Optimized Operational Cost Reduction for an EV Charging Station Integrated With Battery Energy Storage and PV Generation," in *IEEE Transactions on Smart Grid*, vol. 10, no. 2, pp. 2096-2106, March 2019.

[31] C. Luo, Y. Huang and V. Gupta, "Stochastic Dynamic Pricing for EV Charging Stations With Renewable Integration and Energy Storage," in *IEEE Transactions on Smart Grid*, vol. 9, no. 2, pp. 1494-1505, March 2018.

[32] K. Chaudhari, A. Ukil, K. N. Kumar, U. Manandhar and S. K. Kollimalla, "Hybrid Optimization for Economic Deployment of ESS in PV-Integrated EV Charging Stations," in *IEEE Transactions on Industrial Informatics*, vol. 14, no. 1, pp. 106-116, Jan. 2018.

[33] Y. Liao and C. Lu, "Dispatch of EV Charging Station Energy Resources for Sustainable Mobility," in *IEEE Transactions on Transportation Electrification*, vol. 1, no. 1, pp. 86-93, June 2015.

[34] P. Sanchez-Martin, G. Sanchez and G. Morales-Espana, "Direct Load Control Decision Model for Aggregated EV Charging Points," *IEEE Trans Power Syst.*, vol. 27, no. 3, pp. 1577-1584, Nov. 2012.

[35] W. Tushar, C. Yuen, S. Huang, D. B. Smith and H. V. Poor, "Cost Minimization of Charging Stations With Photovoltaics: An Approach With EV Classification," *IEEE Trans. Intell Trans Syst*, vol. 17, no. 1, pp. 156-169, Jan 2016.

[36] D. Rastler, "Technical Specification for a Transportable Lithium-Ion Energy Storage System for Grid Support Using Commercially Available Lithium-Ion Technology," *Electric Power Research Inistiute*, July 2012.

[37] J. Kim and Y. Dvorkin, "Enhancing Distribution System Resilience With Mobile Energy Storage and Microgrids," in *IEEE Transactions on Smart Grid*, vol. 10, no. 5, pp. 4996-5006, Sept. 2019.

[38] G.K. Zaher, M.F. Shaaban, Mohamed Mokhtar, H.H. Zeineldin, "Optimal operation of battery exchange stations for electric vehicles", *Electric Power Systems Research*, vol. 192, pp. 0378-7796, December 2020.

[39] D. L. Applegate, R. E. Bixby, V. Chvatal, and W. J. Cook, *The Traveling Salesman Problem: A Computational Study*. Princeton, NJ: Princeton Univ. Press, 2006, pp. 93-105.

[40] C. J. Eyckelhof and M. Snoek, "Ant Systems for a Dynamic TSP," *Ant Algorithms Lecture Notes in Computer Science*, vol 2463, pp. 88–99, Aug. 2002.

[41] Akandwanaho, Stephen & Adewumi, Aderemi & Adebiyi, Ayodele. "Research Article Solving Dynamic Traveling Salesman Problem Using Dynamic Gaussian Process Regression," *IMA Journal of Applied Mathematics*. vol 2014. , pp. 10-115, Aug 2014.

[42] C. Archetti, D. Feillet, A. Mor, and M. Speranza, "Dynamic traveling salesman problem with stochastic release dates," *European Journal of Operational Research*, vol. 280, no. 3, pp. 832–844, May 2020.

[43] Chang, Tsung-Sheng & Wan, Yat-wah \& Ooi, Wei Tsang. "A stochastic dynamic traveling salesman problem with hard time windows". *European Journal of Operational Research*. vol. 198, no. 3. pp. 748-759. Nov. 2009.

[44] H. Jula, M. Dessouky, and P. A. Ioannou, "Truck route planning in nonstationary stochastic networks with time windows at customer locations", *IEEE Trans. Intell. Transp. Syst*., vol. 7, no. 1, pp. 51–62, Mar. 2006.

[45] Fajardo, D., & Waller, S. T. "Dynamic Traveling Salesman Problem in Stochastic-State Network Setting for Search-and-Rescue Application".

*Transportation Research Record: Journal of the Transportation Research Board*, vol. 2283, no. 1, pp. 122–130, Jan 2012.

[46] P. Sanchez-Martin, G. Sanchez and G. Morales-Espana, "Direct Load Control Decision Model for Aggregated EV Charging Points," *IEEE Trans Power Syst.*, vol. 27, no. 3, pp. 1577-1584, Jan 2012.

[47] K. Liu, C. Wang, W. Wang, Y. Chen and H. Wu, "Linear Power Flow Calculation of Distribution Networks With Distributed Generation," in *IEEE Access*, vol. 7, pp. 44686-44695, Sept. 2019.

[48] Y. M. Atwa, *Distribution System Planning and Reliability Assessment under High DG Penetration*, University of Waterloo: Waterloo, Ontario, Canada 2010.

[49] E. Lopez, H. Opazo, L. Garcia and P. Bastard, "Online reconfiguration considering variability demand: applications to real networks," in *IEEE Transactions on Power Systems*, vol. 19, no. 1, pp. 549-553, Feb. 2004.

[50] A.P. Mazzini, E.N. Asada, G.G. Lage, "Minimisation of active power losses and number of control adjustments in the optimal reactive dispatch problem", *IET Generation, Transm Distrib*, vol. 12, no. 12, pp. 2897–2904, Oct. 2018.

[51] M.F. Shaaban, M. Ismail, E.F. El-Saadany, W. Zhuang, "Real-time PEV Charging/discharging coordination in smart distribution systems", *IEEE Trans on Smart Grid.* vol, 5. no. 4, pp. 1797-1807, July 2014.

[52] "Nikola One," https://nikolamotor.com/one. Oct. 4, 2020 [Accessed 1 Nov. 2020].

[53] M.O. Hanna, M..F Shaaban, M.H. Ismail. et al. "An optimal energy resource allocation framework for cellular networks with power grid interruptions". *Wireless Networks*, vol. 26, pp. 4189–4205, Aug 2020.

[54] Masters, G. *Renewable and Efficient Electric Power Systems* (2nd ed.). Hoboken: Wiley, pp. 1-118, 2013.

[55] H. Abdeltawab and Y. A. I. Mohamed, "Mobile Energy Storage Sizing and Allocation for Multi-Services in Power Distribution Systems," in *IEEE Access*, vol. 7, pp. 176613-176623, Sept. 2019.

[56] "SODA, Solar Energy Services for Professionals." http://www.soda-is.com/eng/index.html March. 1, 2021. [April. 4, 2021].

[57] "IESO. Market & System Reporting," https://www.ieso.ca/en/Power-Data/Data-Directory. Jan. 4, 2021. [March. 4, 2021].

## Vita

Mohamed M. Elmeligy was born in Monufia, Egypt, in 1997. He received his primary and secondary education in Ras Al-Khaimah, UAE. He received his B.Sc. degree in Electrical and Electronic Engineering from Al Ghurair University in 2019.

In September 2019, he joined the Electrical Engineering master's program in the American University of Sharjah as a graduate teaching and researching assistant. His research interests include power systems, electric transportation, storage systems, demand side management and Smart Grid.